UNCLASSIFIED

SECURITY CLASSIFICATION OF THIS PAGE (When Data Entered)

AD-A196 870

REPORT DOCUMENTATION PAGE

READ INSTRUCTIONS BEFORE COMPLETING FORM

1. REPORT NUMBER: AFIT/CI/NR 88- 69
2. GOVT ACCESSION NO.
3. RECIPIENT'S CATALOG NUMBER

4. TITLE (and Subtitle): UTILITY OF PARTICLE PRECIPITATION DATA AS AN INPUT TO THERMOSPHERIC DENSITY MODELS FOR SATELLITE ORBITAL ANALYSIS
5. TYPE OF REPORT & PERIOD COVERED: MS THESIS
6. PERFORMING ORG. REPORT NUMBER

7. AUTHOR(s): KELLY JON HAND
8. CONTRACT OR GRANT NUMBER(s)

9. PERFORMING ORGANIZATION NAME AND ADDRESS: AFIT STUDENT AT: UTAH STATE UNIVERSITY
10. PROGRAM ELEMENT, PROJECT, TASK AREA & WORK UNIT NUMBERS

11. CONTROLLING OFFICE NAME AND ADDRESS
12. REPORT DATE: 1988
13. NUMBER OF PAGES: 72

14. MONITORING AGENCY NAME & ADDRESS (if different from Controlling Office): AFIT/NR, Wright-Patterson AFB OH 45433-6583
15. SECURITY CLASS. (of this report): UNCLASSIFIED
15a. DECLASSIFICATION/DOWNGRADING SCHEDULE

16. DISTRIBUTION STATEMENT (of this Report): DISTRIBUTED UNLIMITED: APPROVED FOR PUBLIC RELEASE

17. DISTRIBUTION STATEMENT (of the abstract entered in Block 20, if different from Report): SAME AS REPORT

18. SUPPLEMENTARY NOTES: Approved for Public Release: IAW AFR 190-1
LYNN E. WOLAVER 19 July 88
Dean for Research and Professional Development
Air Force Institute of Technology
Wright-Patterson AFB OH 45433-6583

19. KEY WORDS (Continue on reverse side if necessary and identify by block number)

20. ABSTRACT (Continue on reverse side if necessary and identify by block number): ATTACHED

DD FORM 1 JAN 73 1473 EDITION OF 1 NOV 65 IS OBSOLETE

UNCLASSIFIED

SECURITY CLASSIFICATION OF THIS PAGE (When Data Entered)

ABSTRACT

The Utility of Particle Precipitation Data as an Input to Thermospheric Density Models for Satellite Orbital Analysis

by

Kelly Jon Hand, Master of Science

Utah State University, 1988

Major Professor: Dr. Jan J. Sojka
Department: Soil Science and Biometeorology

The purpose of this thesis is to determine the relative (compared to the Ap index) utility of global hemispheric power (PPE), as measured by the NOAA/TIROS satellite Total Energy Detector (TED) system, in describing magnetospherically induced upper thermospheric density perturbations. This was accomplished using satellite accelerometer, satellite orbital, Göttingen Ap, and PPE data from the geomagnetically active period of March 20th to April 10th, 1979.

The first part of the study used Air Force Geophysics Laboratory (AFGL) satellite accelerometer thermospheric density data to determine the correlation between it and the PPE. This was then compared to the density data correlation with the Göttingen Ap. The data was scaled to optimize the meaning and linearity of the correlation coefficients and to emphasize any density fluctuations due to geomagnetic variations. The time series cross-correlation produced about a 6-hour lagged response in obtaining maximum correlation.

This study demonstrated the potential of PPE to be a more useful parameter than Ap. This conclusion considers the potential operational availability of PPE as well as its disadvantage in spatial coverage when compared to the global coverage of Ap. In spite of the disadvantage, PPE correlated just as well with satellite drag perturbations as did Ap. It is suggested that an improved PPE be developed by supplementing the NOAA/TIROS PPE data with other PPE type data such as from DMSP. The hypothesis is that the improved PPE should surpass the Ap as a magnetospheric heat input parameter.

The second part of the study used a semianalytic orbital ephemeris generator, which used a Jacchia 70 upper atmospheric density model (binned using Ap), to test the relative usefulness of the Ap and PPE parameters in determining satellite ephemerides. These two parameters were used as the geomagnetic indices of the density model. The conclusion reached was that the difference between the two parameters was insignificant. This further demonstrated the potential of PPE. However, it was recommended that a more significant test of this potential would be to use a PPE-binned atmospheric model in the drag calculations.

(72 pages)

THE UTILITY OF PARTICLE PRECIPITATION DATA AS AN INPUT TO THERMOSPHERIC DENSITY MODELS FOR SATELLITE ORBITAL ANALYSIS

by

Kelly Jon Hand

A thesis submitted in fulfillment
of the requirements for the degree

of

MASTER OF SCIENCE

in

Soil Science and Biometeorology

Approved:

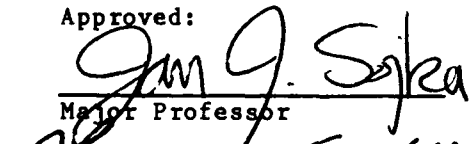

Major Professor

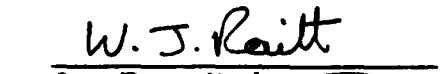

Committee Member

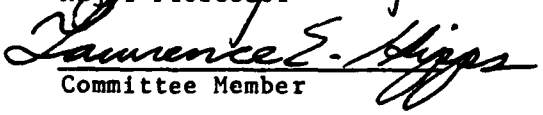

Committee Member

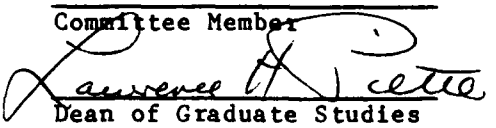

Dean of Graduate Studies

UTAH STATE UNIVERSITY
Logan Utah

1988

ACKNOWLEDGEMENTS

This research was supported by an Air Force OFSR grant to the Center for Atmospheric and Space Sciences. Travel funding was also provided by the Air Force Institute of Technology.

I extend my sincere gratitude to Dr. Jan J. Sojka for his guidance and positive support throughout this research. His practical and theoretical advice have made me a much better student of the space environment.

I would also like to thank Susan Sojka and Beth Wilding for their assistance in the final preparation of this thesis.

I extend my sincere thanks to Dr. Dave Evans, research physicist at the Space Environment Laboratory in Boulder, Colorado, who first guided me in the direction of this research and provided the PPE data.

To Frank Marcos, ionospheric physicist at Air Force Geophysics Laboratory, I convey my heartfelt thanks for his assistance in providing me with the satellite accelerometer data and in assisting me in its correct interpretation.

To Dr. Joseph Liu, Astrophysicist at Air Force Space Command, I would like to express my thanks for his guidance in the orbital analysis study and his help in interpreting the results. Thank you also to Lt. Col.Sundberg for allowing the use of his staffs' expertise and the orbital model which was used in this study. Finally, a special thanks to Lori McCarter for the time and effort she took in running the orbital model.

Thanks also to Don Thompson for his helping me with the Harris and making his plotting software available to me.

Above all to my wife Cindy--thank you for your understanding and loving support through this whole project.

Kelly Jon Hand

TABLE OF CONTENTS

LIST OF TABLES

LIST OF FIGURES

ABSTRACT

The Utility of Particle Precipitation Data as an Input to Thermospheric Density Models for Satellite Orbital Analysis

by

Kelly Jon Hand, Master of Science

Utah State University, 1988

Major Professor: Dr. Jan J. Sojka
Department: Soil Science and Biometeorology

The purpose of this thesis is to determine the relative (compared to the Ap index) utility of global hemispheric power (PPE), as measured by the NOAA/TIROS satellite Total Energy Detector (TED) system, in describing magnetospherically induced upper thermospheric density perturbations. This was accomplished using satellite accelerometer, satellite orbital, Göttingen Ap, and PPE data from the geomagnetically active period of March 20th to April 10th, 1979.

The first part of the study used Air Force Geophysics Laboratory (AFGL) satellite accelerometer thermospheric density data to determine the correlation between it and the PPE. This was then compared to the density data correlation with the Göttingen Ap. The data was scaled to optimize the meaning and linearity of the correlation coefficients and to emphasize any density fluctuations due to geomagnetic variations. The time series cross-correlation produced about a 6-hour lagged response in obtaining maximum correlation.

This study demonstrated the potential of PPE to be a more useful parameter than Ap. This conclusion considers the potential operational availability of PPE as well as its disadvantage in spatial coverage when compared to the global coverage of Ap. In spite of the disadvantage, PPE correlated just as well with satellite drag perturbations as did Ap. It is suggested that an improved PPE be developed by supplementing the NOAA/TIROS PPE data with other PPE type data such as from DMSP. The hypothesis is that the improved PPE should surpass the Ap as a magnetospheric heat input parameter.

The second part of the study used a semianalytic orbital ephemeris generator, which used a Jacchia 70 upper atmospheric density model (binned using Ap), to test the relative usefulness of the Ap and PPE parameters in determining satellite ephemerides. These two parameters were used as the geomagnetic indices of the density model. The conclusion reached was that the difference between the two parameters was insignificant. This further demonstrated the potential of PPE. However, it was recommended that a more significant test of this potential would be to use a PPE-binned atmospheric model in the drag calculations.

(72 pages)

CHAPTER I

INTRODUCTION

In the last twenty years, work in the area of upper atmospheric modeling has produced an increasing knowledge of the physical processes which govern the wind, temperature, density, composition, and electrical properties which are characteristic to this region of space. However, until recently there has been little progress in the area of thermospheric density modeling in conjunction with energy input due to magnetospheric processes.

The traditional geomagnetic variable used as input to the various empirical models has been the Ap (or Kp) index. Recent analysis of the potential of a new parameter related to auroral particle deposition energy [Maeda et al., 1984] has demonstrated a much more intimate connection with the physical processes taking place in the high-latitude thermosphere. The purpose of this study is to determine the role of this energy input in thermospheric density dynamics through the study of observed satellite orbital drag data as it relates to perturbations due to atmospheric density fluctuations.

The hypothesis of this thesis is that particle precipitation energy (PPE) data will improve the modeling of the Earth's upper atmospheric densities as demonstrated through the analysis of actual and modeled satellite orbital drag data.

In order to test this hypothesis, this thesis consists of two general studies.

The first study compares how well the PPE parameter correlates with satellite accelerometer data. This analysis involves a

comparison between intensity fluctuations in particle energy deposition and fluctuations in satellite acceleration due to thermospheric density fluctuations. The corresponding PPE correlation coefficient will be compared to the Ap correlation coefficient which was produced using the same correlation routine. This test will provide insight into the usefulness of the PPE data as it exists in its current form by comparing it to the utility of the more traditional geomagnetic indices.

In addition, an attenuated Ap index is applied to confirm the current understanding of the physical and dynamical processes involved in magnetospheric energy deposition to the thermosphere. It is believed that this type of index provides a better representation of how the thermosphere actually responds to heat input.

With positive results in this first study, recommendations may include building or rebuilding models based on this parameter rather than the current geomagnetic parameters.

The second study analyzes the operational utility of NOAA/TIROS PPE data as applied to Space Command's orbital model data via the Jachia-70 upper atmospheric model. This is done by implementing the appropriate PPE data as a replacement to the Ap index. The utility of this PPE data input will be determined by comparing its results (differences between observed and predicted orbital positions) with the results using the Ap parameter as the model index. The objective of this comparison is to determine the operational utility of PPE in its current form. Since densities are effectively integrated over long path samples, this study would not give as good an indication of actual temporal and spatial effects of particle precipitation as the

first study. Therefore this is mainly an operational applications study.

Chapter II gives a general background of magnetospheric effects on the thermosphere and how auroral particle precipitation is related. Section 2.2 describes how disturbances in the magnetospheric system produce corresponding disturbances in upper atmospheric densities. Section 2.3 discusses how these density enhancements are measured, with Section 2.4 showing how these measurements are applied to thermospheric density modeling. Section 2.5 provides background concerning geomagnetic parameters which are currently applied in modeling studies, with Section 2.6 describing where these indices fall short in their applications. Finally, Section 2.7 introduces the particle precipitation energy parameter by citing past studies which indicate its potential as a more physically viable magnetospheric parameter.

Chapter III deals with the PPE parameter in more detail. Section 3.1 discusses the basic aspects of auroral particle origin and their acceleration and precipitation processes. Section 3.2 presents the instrument used in measuring this parameter and how it measures energetic particles. Finally, Section 3.3 discusses how the raw particle data is used to get an estimate of the hemispheric power input due to these precipitating particles.

Chapter IV summarizes the density ratio correlation study. Section 4.1 presents the background, which introduces the hypothesis that an improved correlation will occur with PPE and how accelerometer data is applied to test this hypothesis. Section 4.2 presents the accelerometer instrumentation. Section 4.3 discusses the

accelerometer data and how density ratio data is obtained from this satellite drag data. Section 4.4 and 4.5 show how the Ap and PPE data were treated so as to maximize the correlation. Section 4.6 gives details of the correlations themselves, and Section 4.7 provides a conclusion.

Chapter V summarizes an operational study done at Space Command with the use of their orbital model. Section 5.2 outlines a similar study conducted by the Directorate of Analysis/Space Command [1983]. This study uses a test which is very similar to the one applied in this thesis. Section 5.3 presents the results of this operational analysis.

Chapter VI contains the conclusions and recommendations which come from this study.

CHAPTER II

GENERAL BACKGROUND

2.1 Introduction

Richmond [1982] summarizes the most important processes which contribute to the heating of the earth's upper atmosphere, and therefore, maintain the density characteristics of the thermosphere: (1) global absorption of EUV and X-ray solar radiation, (2) auroral zone magnetospheric energy input due to mainly Joule heating and, to a lesser extent, particle precipitation, and (3) heating due to turbulence and atmospheric wave dissipation.

This study, since it concentrates on upper atmospheric density perturbations due to magnetospheric heat input, will concentrate on this important aspect of energy input and its effect on the density characteristics of the terrestrial upper atmosphere.

2.2 Magnetospheric Effects on Thermospheric Density

It has been estimated that 60-70% of the amount of upper atmospheric heating from magnetospheric processes comes in the form of Joule heating, with the remaining 30-40% (Evans, private communication, 1988) coming mostly from particle precipitation energy and a minor amount from diffuse precipitation.

Joule heating in the upper atmosphere originates from orthogonal geophysical electric and magnetic fields driving ionospheric plasma through a more abundant neutral gas medium. This plasma motion results in collisions and therefore the production of heat. The rate

of heating is given by [Banks,1980] as $Qj = pE^2$, where p is the Pederson conductivity, which is dependent upon both solar EUV and particle precipitative processes, and E is the applied electric field.

The second major heat input process is that due to direct auroral particle precipitation. The discrete auroral particles are the most significant as far as heat input and ionization of the upper atmosphere is concerned. The particles originate from the plasma sheet, with their energy (.3 to 20 keV) coming from particle acceleration in the near-earth magnetosphere. Electrons are accelerated downward and ions are accelerated upward along the magnetospheric field lines [NASA, 1984]. During magnetospheric substorms, the electrons collide with the upper atmospheric constituents producing enhanced ionization and heating.

Mayr and Volland [1973] have discussed the dynamic effect that magnetospheric storm heat input has on the density characteristics of the thermosphere. Specifically, they note that the mass density responds to this heat input with a strong global enhancement (about 60%) with an associated phase difference of 2 to 8 hours between the equator and pole.

2.3 Upper Atmospheric Density Measurements

Upper atmospheric density models are developed through analysis of data produced by a variety of measurement techniques. The major measurement techniques used today are satellite drag and mass spectrometer studies, incoherent scatter radar measurements of inferred neutral temperatures, and rocket measurements. These

measurements not only reveal the total mass density but also provide a knowledge of the compositional profile of the upper atmosphere.

Jacchia [1959, 1961] has shown, through the use of satellite drag data, that thermospheric densities increase during geomagnetic storms, with these enhancements being reflected in the enhancements of Ap and Kp geomagnetic indices. It has also been shown that the density increases are most pronounced at high latitudes [Jacchia et al., 1967]. This is understandable, since the majority of magnetospheric energy is input into the polar and auroral regions.

2.4 Upper Atmospheric Density Models

Empirical and analytical models are used to study the effect of geomagnetic disturbances on upper atmospheric densities.

For example, a theoretical thermospheric model has been developed [Mayr and Volland, 1973] which assumes the magnetospheric energy input described above. This model, consistent with satellite drag measurements, is basically a three dimensional, two-component model which consistently includes heat conduction, advective energy exchange, ion drag, viscosity, and diffusion. This model consists of two components, one which uses atomic oxygen and molecular nitrogen and a resulting temperature profile, and the other which considers He diffusing through a "fictitious" constituent with a mass corresponding to the mean molecular mass of all the other species.

In the Volland and Mayr model, a representative time for heat input, corresponding to the heat input which would nominally occur during a geomagnetic storm, is used. In the analysis of the storm response, they concluded that energy and diffusive mass transport play

the major role in density, temperature, and compositional perturbations, as seen by satellite drag and compositional studies.

Another important model used in describing perturbations in upper atmospheric densities due to geomagnetic disturbances is the empirical model, which is basically a phenomenological description of the earth's upper atmosphere. Inherent in this characteristic is the simplification of the physical processes which are taking place. They do, however, provide a good first-order approximation of density as a function of time and various parameterized conditions.

One of the most comprehensive and accurate empirical thermospheric models that exists is the MSIS-86 atmospheric density model [Hedin,1987]. This model combines information from satellite drag and composition measurements, incoherent scatter radar data, and various rocket sounding measurements. Specifically, the atmospheric response to magnetospheric energy input is described by an 8-to-10 hour exponential decay in thermospheric density and temperature from storm onset. The latest version of MSIS differs from the earlier ones in that it includes extra coefficients, which are a function of magnetic activity and longitudinally dependent seasonal magnetic activity effects. The model uses a scheme which utilizes a summation of past Ap indices, rather than the daily or three hourly values separately.

Another excellent empirical model which can be used for the same purpose is the Jacchia [1970] model. To represent changing density profiles due to geomagnetic disturbances, this model utilizes a geomagnetic latitude function averaged over local time and other conditions in addition to the geomagnetic Kp index. Input of an

increasing index results in an increasing exospheric temperature, according to an empirically constructed temperature function. This function is then used to construct a corresponding density profile. The amount of temperature increase as a function of Ap is seen in Table 2.1 [Jacchia, 1970].

TABLE 2.1 Temperature Increment as a Function of Ap from the Jacchia Upper Atmospheric Density Model

Ap	T (deg)	Ap	T (deg)
0	0	94	111
15	85	111	210
27	114	132	229
48	145	154	251
67	167	179	279
80	180	207	313

As mentioned above the empirical model oversimplifies and in fact may ignore some physical processes which take place during a geomagnetic storm. For instance, the model may be averaging in the effects that winds have on what appears to be density perturbations detected in the satellite drag data.

Figure 2.1 illustrates the winds contribution to perturbing the drag acceleration of a satellite and the apparent density of the upper atmosphere as determined by the atmospheric-drag equation. This figure was constructed by using density data obtained from the MSIS-86 upper-atmospheric density model and the latest observations of upper-atmospheric winds. An increase in geomagnetic activity as measured by the Ap index (see Section 2.5) corresponds to an increase in density at 200 km, as indicated by the MSIS model. The Ap is the average

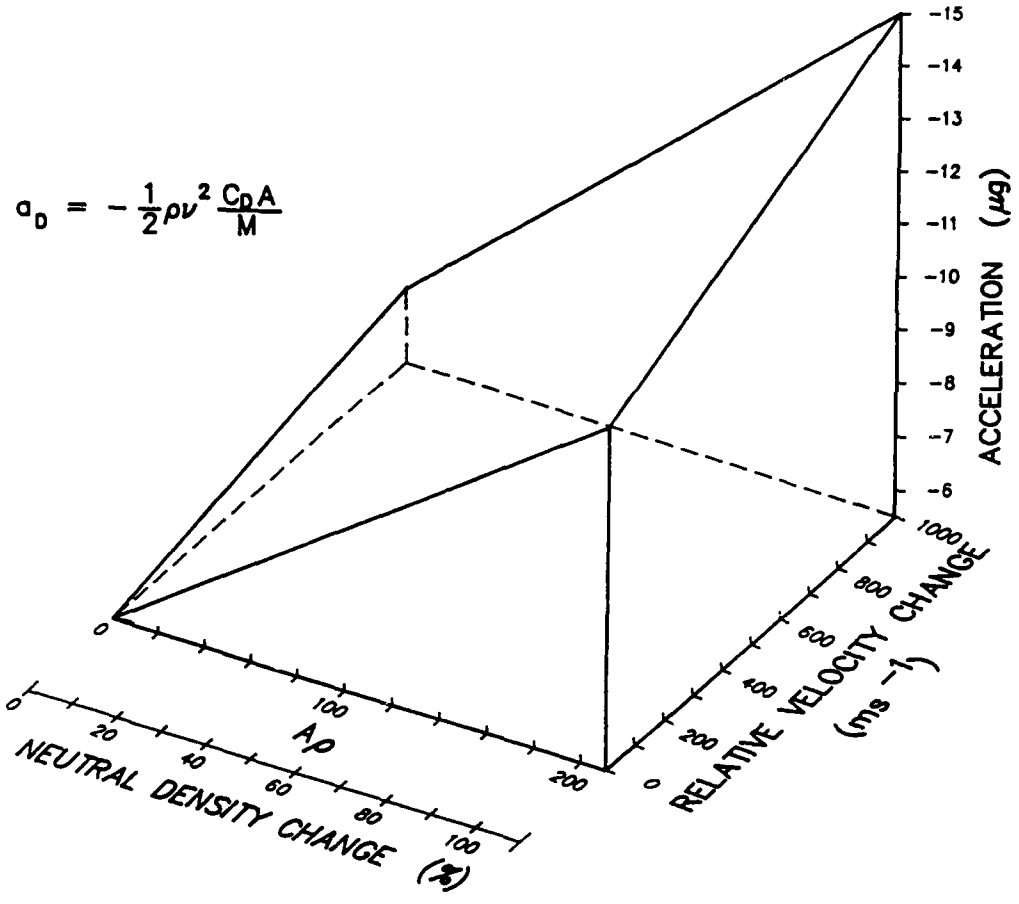

Fig. 2.1 Satellite acceleration as a function of wind and density changes.

value occurring during the preceeding 24 hours. The latitude used was 70 degrees, minimizing the 24-hour factor by the quick response time of this latitudinal region to auroral-heating processes.

The wind data came from accelerometer experiments and represents the winds observed relative to storm conditions at high latitudes Notice that, although wind changes play a role, they still are not as significant in the drag acceleration equation as density enhancements.

The uncertainty in the description of the density profiles as a function of geomagnetic activity not only from the fact that they cannot model winds, but also from the fact that the geomagnetic parameters themselves are not always indicative of the amount of magnetospheric heat input, and therefore density enhancement, taking place. Specifically, the traditional indices used as parameters in these models are either the Kp or Ap geomagnetic index. The next section shows why these geomagnetic parameters give an incomplete picture of energy input into the upper atmosphere.

2.5 Geomagnetic Indices

The indices most commonly used in studying the amount of disturbance in the earth's magnetosphere are the Gottingen Kp and Ap indices. These indices latitudinally and longitudinally average the amount of disturbance in the Earth's geomagnetic field. All these indices are based upon the local, ground based, geomagnetic (H,D,Z) coordinate system or the geographic (X,Y,Z) coordinate system. Figure 2.2 summarizes these two coordinate systems. H is the horizontal component which lies along the local magnetic meridian, and X is the horizontal component lying along the geographic meridian. The

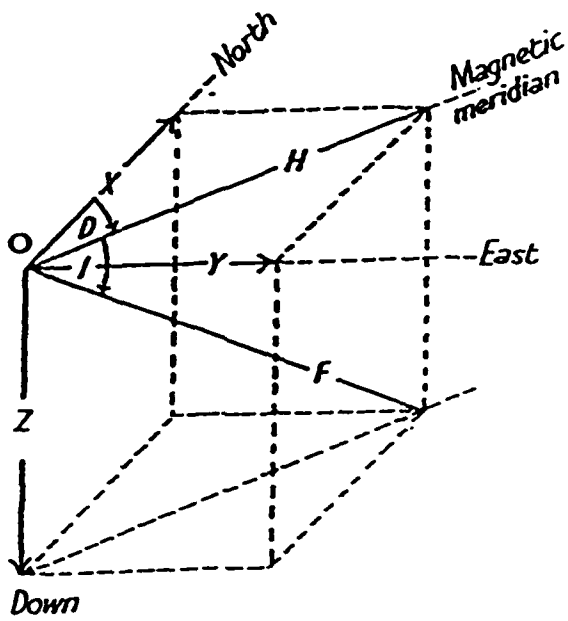

Fig. 2.2 Geomagnetic coordinate systems based upon local magnetic coordinates (H, D, Z), or based upon local geographic coordinates (X, Y, Z).

orthogonal horizontal components are D and Y, with Z as the vertical component in both systems.

The Kp index is a 3-hour indicator of the amount of disturbance in the geomagnetic field. It is a composite of a system of mid-latitude station measurements of the most disturbed local horizontal geomagnetic component. This index uses a quasilogarythmic scale varying through 28 grades.

The Ap index is a linear representation of the amount of disturbance in the geomagnetic field. Ap and Kp are directly interchangeable, as can be seen in Table 2.2.

TABLE 2.2 Ap Index to Kp Index Conversion

Kp	0	1	2	3	4	5	6	7	8	9
Ap	0	3	7	15	27	48	80	140	240	400

Both Ap and Kp are determined as a function of the number of gamma deviations from an undisturbed geomagnetic field component as measured by a ground magnetometer. A qualitative description of the amount of disturbance is summarized in Table 2.3.

The term "active" traditionally means the Ap above which noticeable ionospheric effects are detected (see Table 2.3).

Table 2.3 Geomagnetic Activity Level as a Function of Ap

1. Quiet: Ap = 0-7
2. Unsettled: Ap = 8-14
3. Active: Ap = 15-29
4. Minor Storm Ap = 30-49
5. Major Storm Ap = 50-100
6. Super Storm Ap = 100-400

In addition to the Göttingen Ap, the Air Force uses western-hemisphere magnetometer stations to produce a "pseudo-realtime" Ap. This index is required since the Air Force needs a real-time geomagnetic index for operational use. Statistics are applied to this index to produce an improved representation of the Göttingen Ap. In addition, the index is weighted to emphasize auroral latitude effects [Krause, private communication, 1988].

2.6 Inherent Problems with Geomagnetic Indices

The major geomagnetic indices used by empirical models have been described. Some inherent problems remain when using these geomagnetic indices as parameters to describe the intensity of a given geomagnetic storm as applied to these models and therefore to describe the subsequent density perturbation in the earth's upper atmosphere. The following is a summary of the limitations of these indices as pointed out by Baumjohann [1986].

In general, both indices are constructed from measurements by stations which have uneven spatial distributions. Because of this it is very difficult to determine the maximum level of disturbance of a given geomagnetic storm, and, therefore, overestimation of a storm could take place.

Also, the Kp and therefore the Ap indices are very poor choices as parameters in describing the amount of heat input to the auroral zones. This is due to the fact that the stations measuring this index are equatorward of the auroral oval, and, therefore, a given auroral substorm could be missed.

Another major problem concerns interpreting Kp or Ap due to the motion of the auroral oval. This problem results from one of three possible phenomena. Firstly, it may be possible that there is an actual increase in the current in the auroral zone. Secondly, the auroral zone may be moving toward the observatory. Finally, both of the above processes may be occurring simultaneously.

An additional problem arises with the operational application of the Ap and Kp indices. As mentioned in Section 2.5, Göttingen Ap values are not available in real time and are therefore unavailable for "real time" use. Hence the U.S. Air Force uses a series of western hemispheric stations in real time and weights this Ap value to reflect the statistical Göttingen Ap and high latitude processes. This step obviously compounds an already large error (see above) by adding a hemispheric gap to the coverage of a particular geomagnetic event.

It is obvious that the traditional geomagnetic indices, although connected with the physics of the magnetospheric system, are far removed from providing a consistent interpretation of what is happening in the case of heat input into the auroral zone. So what parameter is available today which may help to fill this gap? This thesis will examine this question by determining the relative utility of the particle precipitation energy (PPE) parameter.

2.7 Potential of Particle Precipitation as a Magnetospheric Parameter

As described in Section 2.2 the majority of heat input to the upper atmosphere comes in the form of Joule dissipation and the

remainder in the form of particle energy dissipation. Also mentioned was that the amount of Joule heat input into the upper atmosphere is proportional to the Pedersen conductivity and the resultant vector electric field. Since particle precipitation is not obviously reflected in that electric field, the only other possibility is to relate particle precipitation to the Pedersen conductivity. This connection was mentioned in general in Section 2.1. More specifically, it arises because the Pederson conductivity is a function of the ionization rate or the energy deposition rate associated with auroral precipitation. One can therefore conclude that Joule heating and particle precipitation are coupled phenomena [Rees et al., 1983]. If this is true, since Joule heating is the main heat input source and direct particle precipitation is considered the second major heat source, there should be a high correlation between thermospheric density enhancements and particle precipitation energy.

Two excellent studies have been conducted to confirm the potential of this parameter in describing the effects of magnetospheric disturbances on upper atmospheric densities.

Maeda et al. [1984] utilized energetic particle observations made by the NOAA/TIROS polar orbiting satellites as a heat-input parameter in an empirical model constructed by a combination of Millstone Hill Incoherent Scatter Radar electric field data and these same particle observations. In the model the amount of magnetospheric heat input into the upper atmosphere is governed by a corresponding particle energy index. To test the model, a seven-day period in which a geomagnetic storm occurred was used. The results of the study showed

a high correlation between exospheric temperature and the activity level.

In addition to this study, Coster and Gaposchkin [1987] evaluated how well the effects of different atmospheric parameters were being modeled, among these was the NOAA/TIROS particle precipitation index. In their study Millstone and Altair radars were used to track two spherical satellites. Their results showed that the precipitation index was associated with atmospheric drag acceleration.

This thesis proceeds on the possibility that particle precipitation energy may have a greater potential in describing thermospheric density enhancements than the traditional geomagnetic parameters and therefore may have higher utility in satellite atmospheric drag applications.

CHAPTER III

AURORAL PARTICLE PRECIPITATION

This chapter deals with the physics, measurement, and data associated with auroral particles of energy range .3 and 20 KeV. This energy range is used because the majority of the energy which is input into the auroral zones is at least indirectly connected with particles precipitating with these characteristic energies and is, therefore, the major contributor to magnetospheric-induced density perturbations of the upper atmosphere.

3.1 Introduction

This section studies the rudimentary aspects of the magnetospheric origin, as well as acceleration and precipitation processes associated with auroral particles. For a more detailed discussion see Cosmical Geophysics [1973].

3.1.1 Magnetospheric Origin and Acceleration Processes

In general, auroral particles are defined as those particles which originate in the magnetosphere and possess energies from 100 eV to 100 KeV. These particles obtain this characteristic energy range from various acceleration processes, precipitate in the upper atmosphere, and deposit their energy, producing the various perturbative phenomena attributed to dynamic magnetospheric processes.

Exactly where do these particles come from? They originate mainly from corpuscular radiation (mainly electrons and protons) which emanates from the sun (commonly known as the solar wind) or thermal

plasma less than or equal to leV from the ionosphere. A small fraction of the solar wind plasma enters the magnetosphere (the exact mechanism is not fully understood) through a merging of the interplanetary magnetic field with the Earth's geomagnetic field. The whole system approximates a magnetohydrodynamic generator which has the solar wind as its plasma source and the geomagnetic field as the interacting magnetic field, with the ionosphere providing a load for the generator.

More specifically, the region within this "generator" where precipitating auroral particles (see Sections 2.2 and 2.7) originate is the plasma sheet of the magnetotail. Figure 3.1 shows how the plasma sheet appears within the magnetospheric system.

The plasma sheet has a "quiet" characteristic plasma density of about 0.1-10 cm-3. The electron population has a typical energy of about 1 KeV and a range between 1 and 10 KeV. The temperature of this region approximates a Maxwellian distribution and averages about 10 million degrees Kelvin. The proton population differs from the electron characteristics in that the proton population has a greater maximum energy (by a factor of about 4). For both populations the angular distribution is basically isotropic during undisturbed periods.

It has been observed that during disturbed conditions the plasma within the plasma sheet becomes energized to about 1 KeV, but since this is not enough to account for the observed energy of auroral particles it is obvious that there are acceleration processes other than kinetic heating taking place. Some of the major processes believed to be involved in this acceleration are (1) neutral region

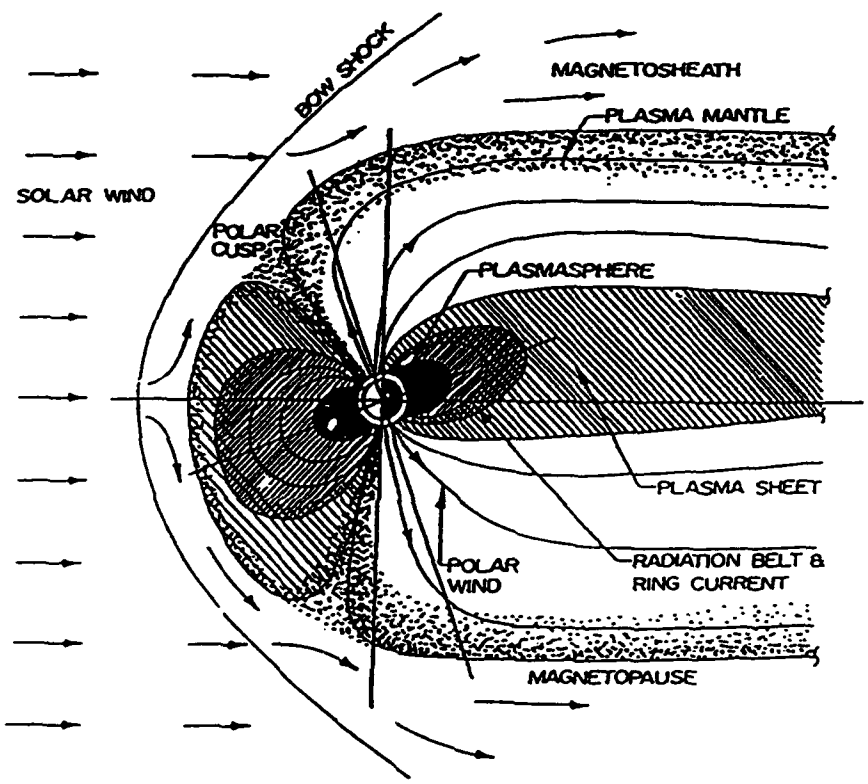

Fig. 3.1 Cross section of the magnetosphere. From Bahnsen (1978).

acceleration, (2) field line merging, (3) Fermi acceleration, (4) betatron acceleration, (5) transverse electric field acceleration, and (6) parallel field acceleration [Cosmical Geophysics, 1973].

3.1.2 Precipitation Processes

The two major precipitative mechanisms connected with energy input into the Earth's upper atmosphere due to magnetospheric processes are atmospheric ionization and thermal energization, with a relatively minor contributor being atmospheric excitation. The ionization and excitation collisional processes store energy electrochemically or radiate through secondary recombination processes, but eventually the energy must be either thermally absorbed by the atmosphere or radiated as electromagnetic radiation (the aurora).

3.2 Auroral Particle Measurement Techniques

There are three major techniques used in measuring the characteristic energy of precipitating auroral particles: (1) in situ rocket and satellite measurements, (2) satellite auroral imagers, and (3) ground-based optical sensors. Direct measurement is by use of the in situ rocket and satellite detector. By integrating the energies of particles detected by the NOAA/TIROS satellite Space Environment Monitor (SEM) a method was devised [Evans, private communication, 1987] to estimate the amount of power that is being input into the Earth's upper atmosphere due to magnetospheric processes. The energy may also be measured more indirectly by use of an auroral imager (eg. Dynamics Explorer, [Frank et al., 1981]) or a ground-based optical sensor (e.g., meridional scanning photometer, [Romick, 1976]).

Since this thesis uses data from the NOAA/TIROS SEM, this section will be devoted to a discussion of this particular auroral particle monitor. The major aspects of the NOAA/TIROS Space Environment Monitor (SEM), and in particular the Total Energy Detector on board this series of spacecraft, are presented (for a detailed discussion the reader is referred to Seale and Bushnell, [1987]).

The TIROS-N SEM measures the near-earth charged particle environment. This 850 km altitude satellite system allows sampling of energetic particles precipitating in the auroral zones. This is done by way of three SEM monitors, a Total Energy Detector (TED), a Medium Proton and Electron Detector (MEPED), and a High Energy Proton and Alpha Detector (HEPAD). The TED is the source of the data used in this thesis.

The TED measures electrons and positive ions (assumed to be protons) in the energy range of .3 to 20 KeV. Four separate detector units measure these particle populations in two different directions, one parallel and the other 30 degrees relative to the magnetic field line at high latitudes.

> The detector assembly uses a cylindrical-plate electrostatic analyzer with about 13% energy resolution. A voltage difference is impressed on the analyzer plates. The polarity of this voltage determines whether positively charged ions or electrons are detected. The magnitude of this voltage selects a band of particle energies centered at some energy E, for which the particles are passed through the analyzer.
>
> The analysis is followed by a 'spiraltron' type channel electron multiplier which produces a relatively large pulse of electrons for input particles of either positive or negative charge, independent of particle energy. It does this in an electron avalanche of secondary emission. Preacceleration fields of appropriate polarity are applied between the electrostatic analyzer exit and the spiraltron cathode to ensure that even the lowest energy particles produce enough electrons at the cathode surface to be counted. The channel electron multiplier counts those

charged particles which have passed through the analyzer. [Seale and Bushnell, 1987].

The four analyzers are mounted in pairs, with each analyser pair measuring the proton and electron directional flux relative to the two angles previously mentioned. One pair views outward, parallel to an earth-centered radial vector, while the other views at an angle 30 degrees relative to this. In a period of two seconds, the detectors alternate sweeping across the electron and proton energy spectrum. The resulting output is the total directional energy flux integrated for both charge species over the entire .3 to 20 KeV range. For a more detailed discussion of the derivation of the total directional energy flux see Seale and Bushnell [1987].

Since the data is measured at 850 km altitude, the data must be manipulated to express what this flux would be at 120 km, the altitude where the particles precipitate. This is done with a geomagnetic field model (IGRF). Figure 3.2 is a schematic of the relationship between the field line and the TIROS-N orbit. Since the magnetic field lines are not radial, large errors would be introduced if this were ignored. It is here that the field model is used. The model basically traces the field to intersect the spacecraft location and then proceeds to intercept the top of the atmosphere at 120 km. Additionally, the model calculates the angle between the geomagnetic field direction and the look direction of the two detectors. These two resulting angles are the two respective local pitch angles. To obtain the pitch angle at 120 km altitude the following relationship is used:

$$\sin \alpha_{120} = \sqrt{B_{120}/B_{850}} \sin \alpha_{850}$$

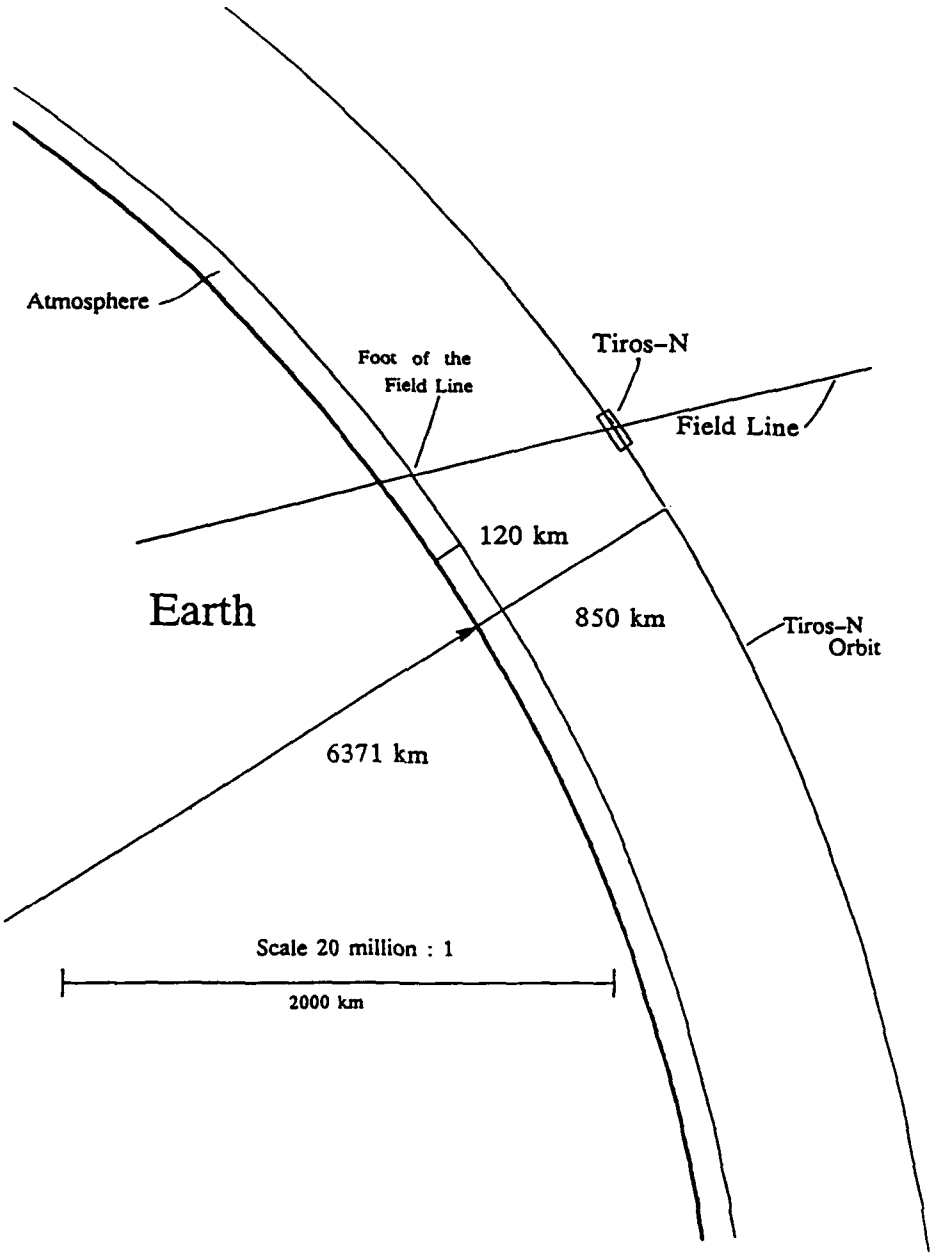

Fig. 3.2 Schematic relationship between a magnetospheric field line and the NOAA/TIROS satellite orbit.

where

α_{850} = pitch angle at the TIROS-N spacecraft at 850 km altitude

α_{150} = pitch angle at 120 km altitude

B_{850} = geomagnetic field strength at the TIROS-N spacecraft at 850 km altitude

B_{120} = geomagnetic field strength at 120 km altitude

The number of particles integrated at the two angles for the two charge species is summed to become the total energy flux.

The latitudes which produce the majority of auroral particle flux are poleward of 40 degrees. Because of this, this instrument includes only these high-latitude regions in its sampling. The resulting error, due to a field inclined to the horizontal, becomes about 13% (1-cos 30 degrees) since the maximum inclination to the horizontal is 60 degrees.

3.3 Total Hemispheric Power Input Data

This section shows how Total Hemispheric Power Input data is obtained [Evans, private communication, 1987].

Due to the dynamic nature of auroral morphology coupled with the Earth's rotation, the dipole nature of the geomagnetic field, and many other complicating factors, obtaining an estimate of a global picture of auroral precipitative power input from a single orbit pass is a nontrivial task. The only way to obtain such an estimate is through statistical correlation. To gain an appreciation of this task, consider what it would be like to take a line of meteorological stations across the 40th parallel at 5 degree longitudinal increments, and from this limited information try to statistically deduce what the

continuous weather picture would be over the entire United States. Fortunately, hemispheric auroral zone dynamics have relatively more symmetric properties than do weather patterns, but this does not lessen the difficulty of this statistical procedure.

To accomplish this, Evans [private communication, 1986] constructed a scheme whereby he ordered energy flux observations over one degree dipole geomagnetic latitude intervals.

> This technique first performs the line integral of the energy flux (weighted by the cosine of the magnetic latitude of the individual measurement) along the satellite trajectory as it passes over the polar regions. This line integral is then corrected for the manner with which the satellite would have sampled a statistical auroral zone during that pass. The validity of this correction assumes that the pattern of auroral particle precipitation takes on a 'generic' shape which depends only upon the level of activity. When done properly, this correction will remove a variety of effects related to the satellite orbits (dependences upon the hemisphere being sampled, the universal time of day that the pass occurred, etc.) and will yield the 'best' estimate of the total amount of energy being deposited into a single auroral zone by the incident particles. Values of power input range from 1.5 Gigawatts per hemisphere during quiet times to more than 300 Gigawatts per during very active times. In the analysis of the NOAA/TIROS data, these estimates of hemispheric power input play the role of an activity index, replacing the more traditional magnetic activity indices.
>
> Estimates of hemispheric power inputs have been computed for every satellite pass in the historical data base; 100,000 passes dating back to late 1978. Individual passes have been sorted into 10 bins depending upon the associated power input, beginning with passes having power inputs below 2.5 Gigawatts and continuing up in a geometric progression to the bin containing the 1% of all passes having power inputs above 96 Gigawatts. The individual local measurements of energy flux made during each pass within a given activity bin, and at the same corrected magnetic latitude and local time location, were averaged together to create a statistical pattern of the global particle energy input appropriate to that level of auroral activity [Evans, private communication, 1986].

This method gives the best estimate of the total amount of energy that is input into an auroral zone hemisphere from magnetospheric processes.

Although this data is the best data available for real time application in estimating the amount of heat input into the thermosphere, there are certain factors inherent in the sampling procedure which limit the accuracy of the estimate. As the estimate is based on purely empirical analysis and the energy input to the hemisphere is so dynamic, the estimate is biased as to when and where the sample is taken.

Additionally, it assumes that the "normal" spatial distribution of energy flux corresponds closely to a statistical auroral oval model. This may not always be the case since large variations may exist in the spatial structure of auroral particle precipitation, which itself may deviate considerably from a given statistical oval. Furthermore, assymmetries in magnetic local time are also known to exist. Taking this into account, a one-pass estimate may misinterpret the global picture, thus implying that more satellite sampling could improve the parameter.

Our current understanding suggests that energy input into the auroral zones exhibits symmetry between hemispheres. To show the degree of interhemispheric symmetry, Figure 3.3 shows plots of hemispheric power over the period tested for the northern (top panel) and southern (bottom panel) hemispheres. This plots hemispheric power input in Gigawatts versus time.

Notice (especially Day 81) that the ratio between hemispheres is not always unity. This suggests that either 1) there is some assymmetry in the system, 2) the dynamics are faster than the sampling

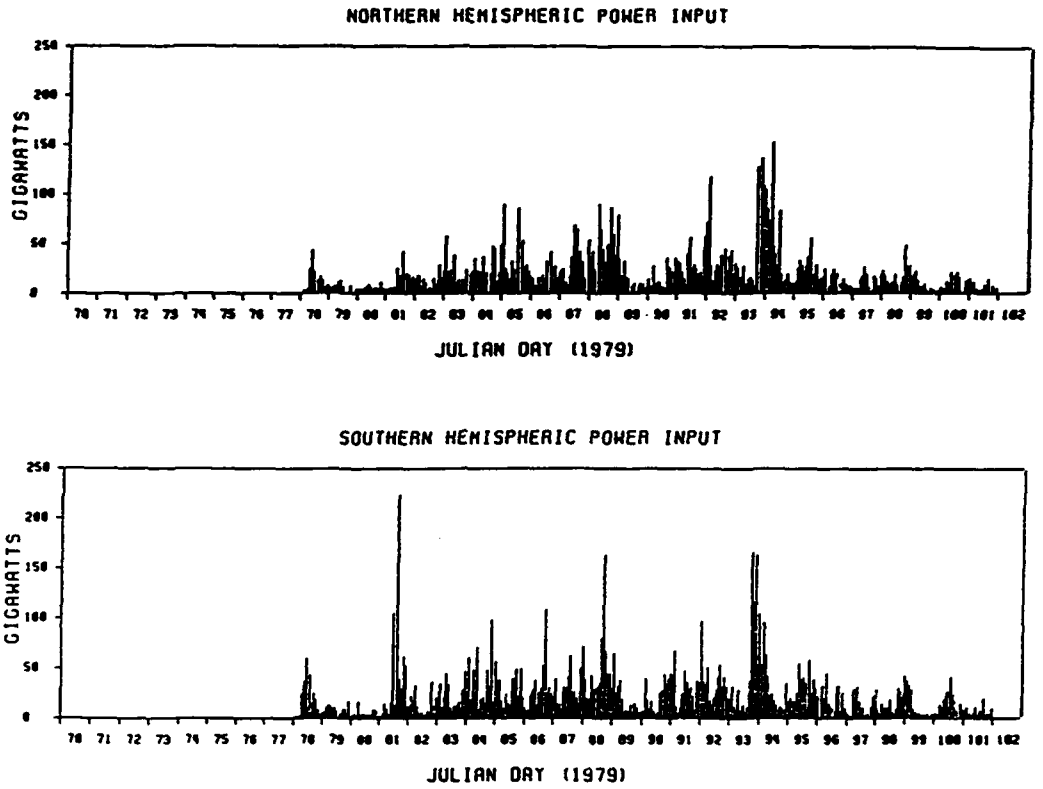

Fig. 3.3 Northern (top panel) and Southern (bottom panel) hemispheric power input (PPE) in Gigawatts versus Julian Days (70-102, 1979).

can keep up with, 3) the statistical oval method is at fault, or 4) a combination of the above. In this study this is partially overcome by combining the two data sets to produce a more global representation. In the next two chapters this combined hemispheric power index is used to accomplish the objective of this thesis.

CHAPTER IV

ACCELEROMETER STUDY

4.1 Introduction

Marcos et al. [1977] have demonstrated the enormous potential of accelerometers in providing an objective means for the determination of the utility of geomagnetic parameters as used in various empirical upper atmospheric density models. These parameters are used by the models to describe thermospheric density response to magnetospheric processes. In their particular case study Marcos determined that the 12-hour average of the Kp provided the best estimate of the description of density perturbations.

Many studies have analyzed the utility of these traditional geomagnetic parameters in describing satellite atmospheric drag fluctuations due to magnetospheric energy-induced density changes and have concluded that a new parameter is needed that is more physically connected with the amount of heat input to the upper atmosphere. One such parameter is particle precipitation energy as measured by the NOAA/TIROS series of spacecraft (see Section 2.7).

As mentioned previously, the objective of this thesis is to determine the utility of in situ energetic particle measurements in describing thermospheric density perturbations. The potential of this parameter was emphasized because these particles are believed to contribute 30-40% of their heat directly into the thermosphere and are believed to be physically connected with the electrodynamic process of

Joule dissipation, which is considered the major magnetospheric heat input source to the Earth's upper atmosphere.

If this is the case, then one should see a statistical correlation between particle precipitation and density perturbations measured by a satellite accelerometer. Furthermore, if this parameter is indeed an accurate representation of the whole physical picture, then one should see a better correlation coefficient with PPE and the density ratio than with Ap and the density ratio. Also, since this is a correlative study, the comparison of the correlation coefficients should provide a viable answer to the relative practical utility of this new parameter as it exists in its present form.

First, the instrumentation of the accelerometer will be presented in order to show how density perturbations are detected by a satellite accelerometer. Next, the density ratio data obtained by the accelerometer will be described. Then, the particle precipitation data (PPE) and the Ap data are described in general and then specifically as to how the data is processed to make a viable correlation. After all the data is presented, the next section will describe the main points concerning the derivation and meaning of a linear-correlation coefficient. Finally, the specific correlation studies will be presented along with the conclusion of the thesis of the relative usefulness of PPE in accessing satellite drag.

4.2 Accelerometer Instrumentation

This section describes the accelerometer instrument and is taken from Air Force Geophysics Laboratory Technical Regulation 78-0003 [Lange, 1977].

The satellite accelerometer consists of a "proof mass" (center) constrained in three axes by electrodes. These electrodes surround the mass on all sides and maintain its null or zero acceleration position. The mass is surrounded by an electronic rebalance loop (see Figure 4.1), giving an output proportional to the acceleration of the mass.

Accelerations detected are not only the orbit track, but cross track as well. This is done by sensing the motion of the proof mass with respect to the instrument case. An electrostatic force is then generated to oppose this motion in the direction of the null position. This force is generated from a d-c potential proportional to the input acceleration. This information is converted to a digital output signal. The signal is converted to a pulse rate and each pulse represents an increment of velocity. The pulses are accumulated in a bi-directional counter for a predetermined period. Subsequently, an output data word represents the average acceleration over the "sample time" period. The data output consists of a single 64-bit word, which describes acceleration, direction, and range information of all three axes.

4.3 Accelerometer Data

The accelerometer data used in this study comes from the Satellite Electrostatic Triaxial Accelerometer (SETA-1) satellite [Marcos, 1984] which sampled from March through April of 1979. The period used in this study was a twenty-day period between March 20 and April 10, 1979. The SETA-1 orbit was sun-synchronous, with the sample data starting at about 20 degrees geographic north at

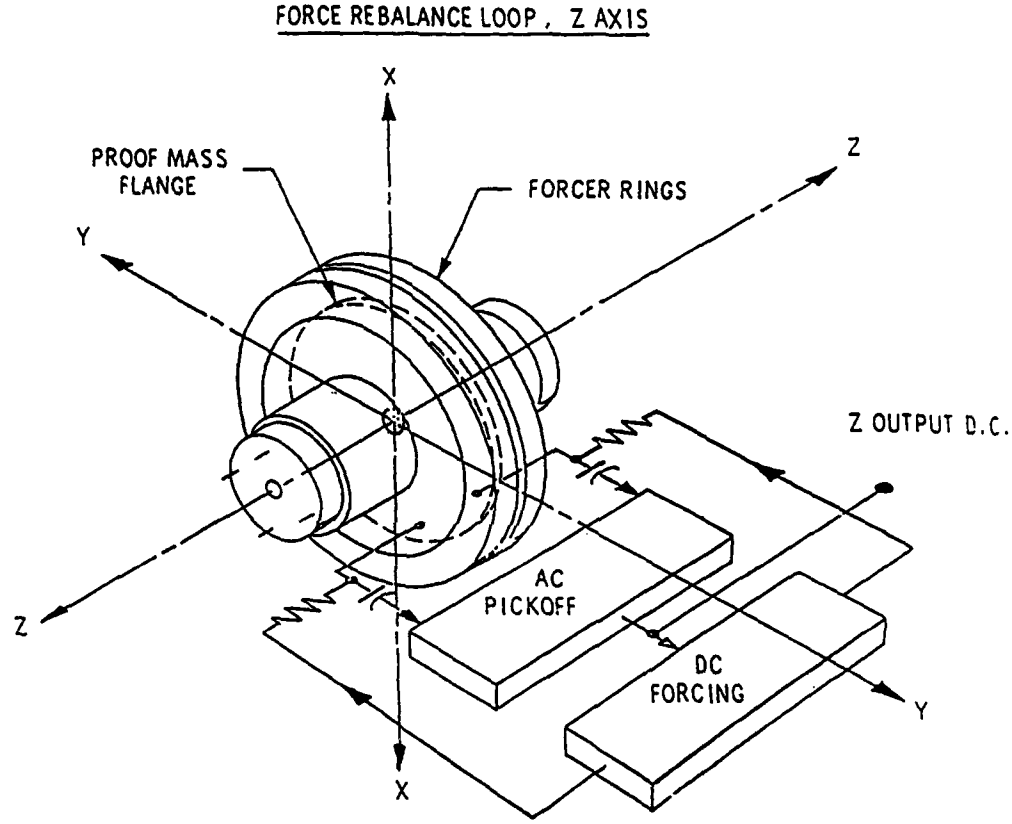

Fig. 4.1 Diagram of the constrainment loop connection to the electrodes within the mechanical assembly.

approximately 200 km altitude on the night side, coming around to about 170 km at its lowest position at about 34 degrees north on the day side, and finally ending at the equator on the dayside at about 180 km. Straight density plots indicate that this sample takes into account about 85% of all the atmospheric drag taking place around each orbit. This is easily understood, as the orbit is slightly elliptical. The northern hemisphere sample contains the lowest altitude in each orbit and produces the most drag [Marcos, private communication, 1988]. The resulting data show the average density taken over the individual orbital periods.

In order to emphasize the affects of magnetospheric variations, the densities detected by the accelerometer were divided by a model reference density where the Kp was set to 0 (same as 0 Ap). The *Jacchia 77 [Jacchia, 1977] empirical* upper-atmospheric density model was used by AFGL to obtain the needed density ratio. This procedure allows one to take into account environmental variations such as solar heating, local time variation, altitude change, etc.

Figure 4.2 (bottom panel) shows the entire sample of density ratio data. The first two days are considered geomagnetically "quiet" (Ap < 15). The corresponding estimate for a "quiet" density ratio level is about .93 to .95. Density ratios vary between .93 during "quiet" to more than 1.21 during disturbed conditions.

The average time between sample periods was 1.488 hours. This time varied throughout the sample period within plus or minus a few minutes. Also, the amount of variation between sample regions was negligibly small (plus or minus a few degrees due to orbit

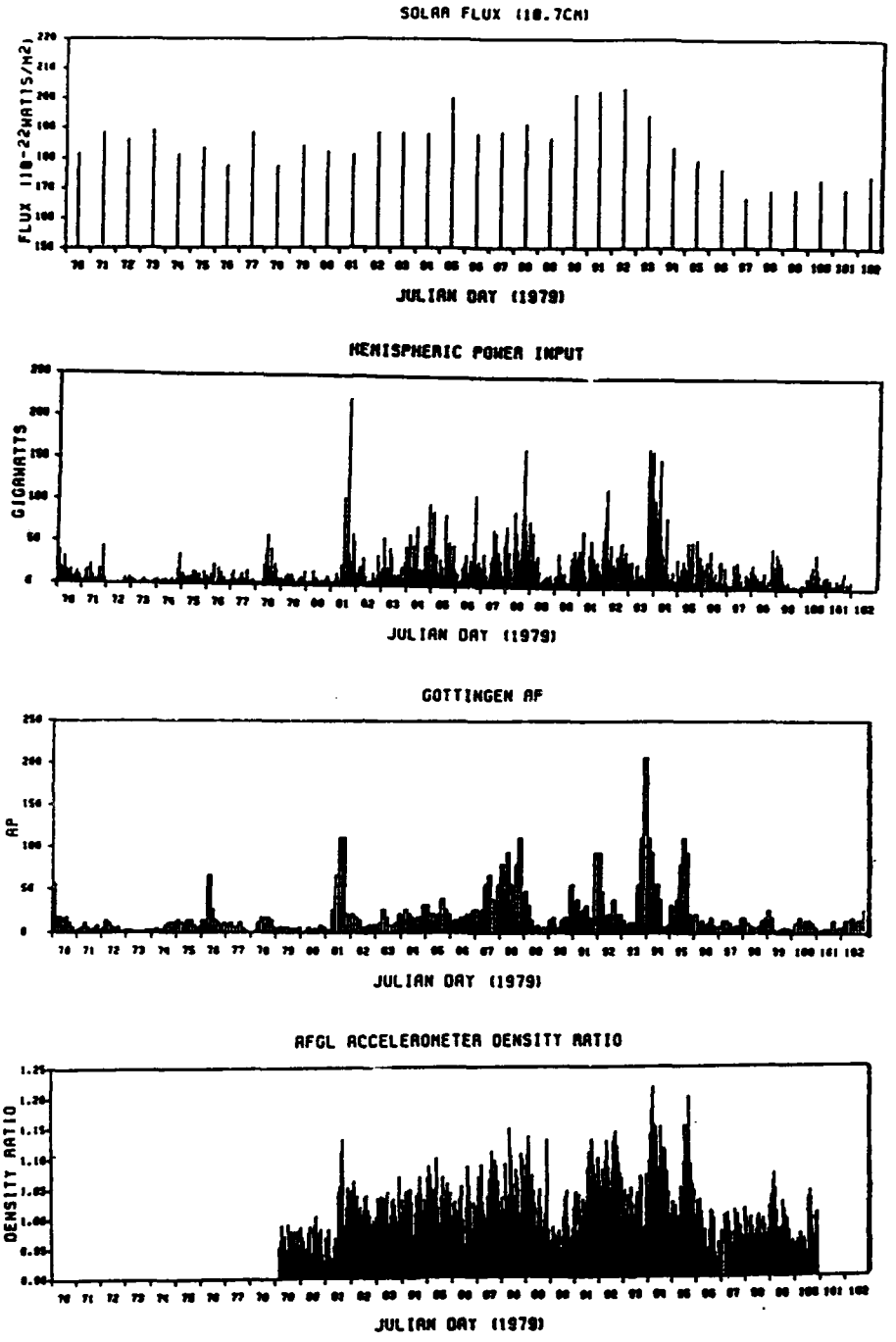

Fig. 4.2 Ottawa 10.7 cm flux (first panel), NOAA/TIROS hemispheric power input (second panel), Göttingen Ap index (third panel), Air Force Geophysics Laboratory satellite accelerometer density ratio data (bottom panel) for the entire sample period (Julian days 1979).

perturbation), allowing the correlation to be done as a time series (see Section 4.5).

4.4 Ap and Particle Precipitation Data

In order to do an appropriate time series correlation between the accelerometer data and the Ap and PPE parameters, the two parameters had to be matched to the accelerometer sample times. This was done by first matching the Ap values to the appropriate PPE sample times, finding the square root (see section 4.5) of these values, and finally linearly interpolating to the accelerometer sample end times. In addition to the density data described above, Figure 4.2 shows the raw solar flux at 10.7 cm (top panel), particle precipitation energy (second panel), and the Göttingen Ap index (third panel) during the entire sample period. Also included are nine days of flux, PPE and Ap data preceding the sample period. These days are included to provide adequate parameter history preceding the sample period. Notice in particular the relatively quiet magnetospheric conditions preceeding and including the first two days of the period of interest.

4.5 Optimization of Parameter Correlations

To provide a viable comparison between Ap and PPE as parameters in describing thermospheric density perturbations and to optimize the physical correlation between them and the density ratio, the relationship between the two parameters must be determined, and the effect that an increase in the value of the parameters has on the density ratio at the appropriate altitude must be estimated.

The first objective, to establish the relationship between the two parameters, was accomplished by correlating Ap with PPE over the short and long term. Here, short term means over the sample period (days 79 through 100, 1979) and long term means over an entire year (1979). Figure 4.3 shows a scatter plot of scaled PPE versus Ap for these two periods along with the corresponding correlation coefficients. Notice that although the correlation is approximately linear, the scatter is tremendous; a variation in one does not always describe a variation in the other.

The second objective, the determination of the effect that changes in the two parameters have on the density ratio, was accomplished using an empirical model (MSIS 86 [Hedin, 1987]) where an increasingly intense Ap was input into the model. This served to determine what the resulting density change would be, given a certain level of geomagnetic activity. The corresponding change in the density at 200 km was then computed as a function of increasing Ap (200 km is roughly the altitude of the satellite accelerometer). In this particular case the 10.7 cm flux (solar energy input) was consistent with the average observations during the sample period. The resulting density was then divided by what the model would expect based on an Ap of 0, thus providing the needed density ratio. A plot was constructed which showed the relationship between the Ap and the density ratio. From inspection it looked as if the functional relationship was that of a square root; therefore, the plot was made with the abscissa being the square root of Ap.

Figure 4.4 is the plot of the density ratio versus the square root of the increasing 24-hour average Ap. As one can see from this

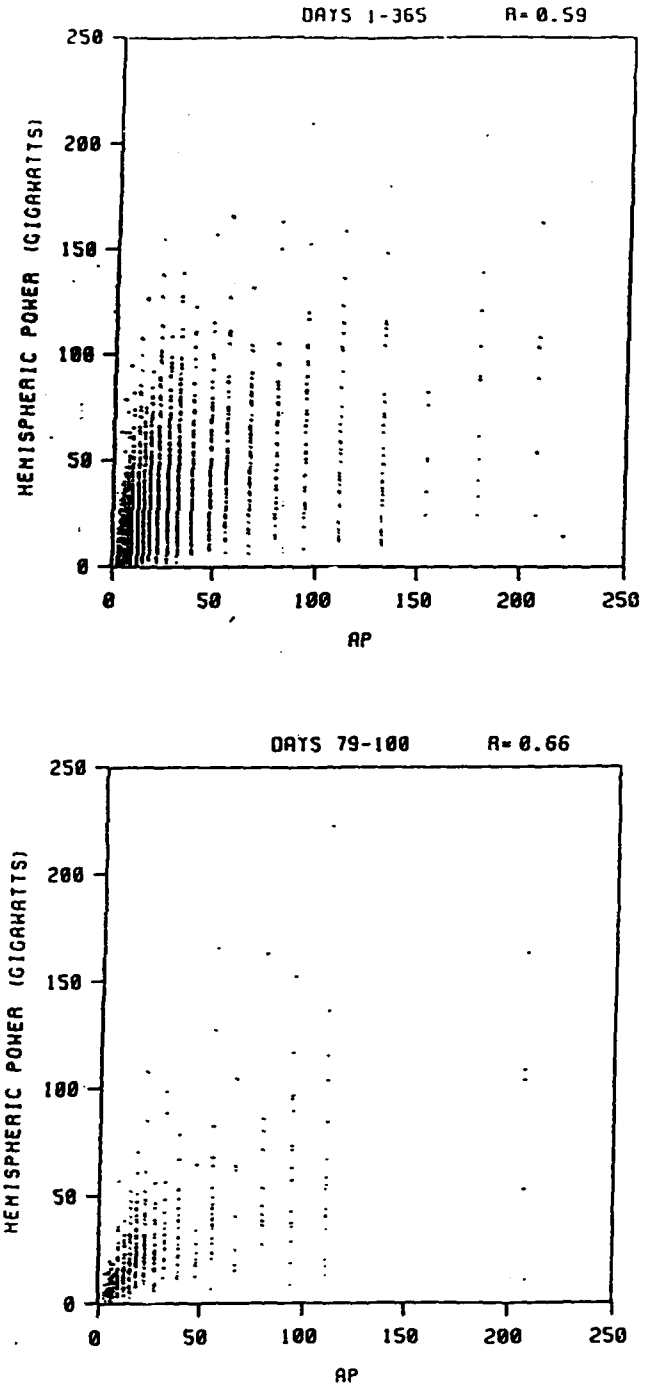

Fig. 4.3 Scatter plot of hemispheric power input verses Ap for the entire year 1979 (top panel) and for Julian days 79 - 100 (bottom panel).

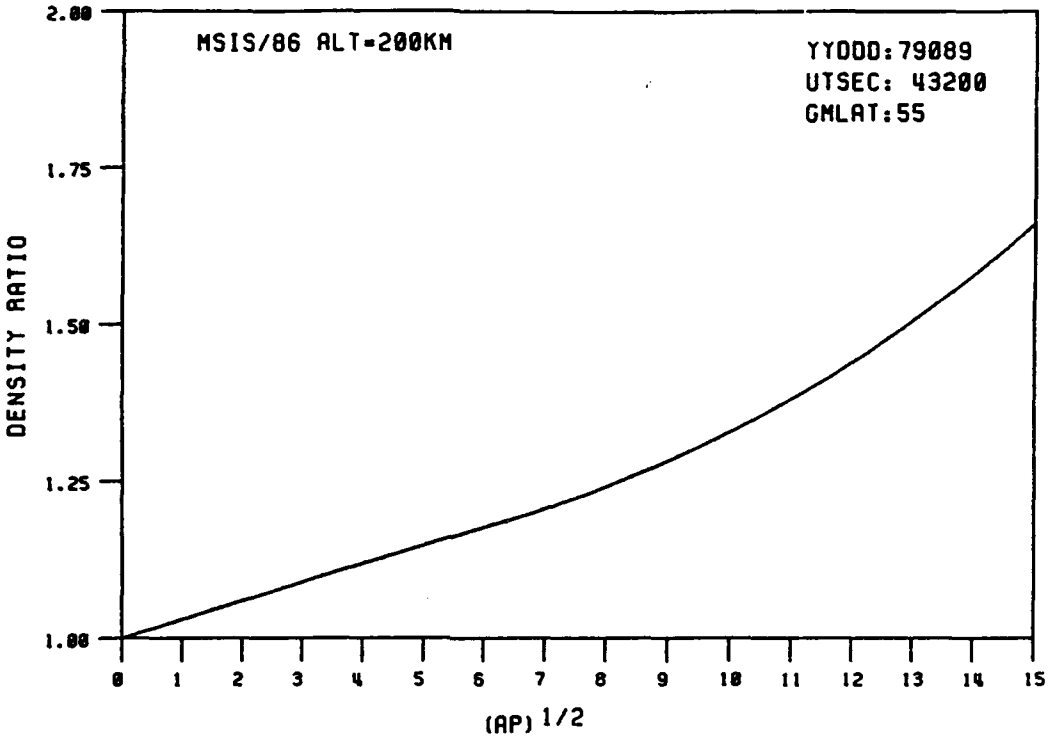

Fig. 4.4 Density ratio (MSIS 86) versus the square root of corresponding Ap index at 55 degrees geomagnetic north latitude, 200 km altitude, at local noon on Julian day 89.

figure, the square-root relationship exists up to an Ap of 100. The figure also shows a lack of linearity as an Ap of 100 is exceeded. This fact is ignored in this correlative study as only one three-hourly value exceeds an Ap of 111. Therefore, because of the approximate linear relationship between Ap and PPE and the square-root relationship between increasing Ap and the corresponding density ratio, this study uses the square root of PPE and Ap when performing linear correlations with the accelerometer-measured density ratios.

4.6 Data Correlations

This section describes the data-analysis method used to make a viable comparison between correlation coefficients possible. The section is divided into two parts. The first study uses the raw interpolated Ap and PPE data, while the second uses a time-weighted Ap [Wrenn, 1987].

4.6.1 Correlations Using Interpolated PPE and Ap Data

Particle precipitation data was obtained for a period of 24 days [Evans, Private Communication, 1986]. The range of this period covers the entire density sample, with an overlap of a few days either side of the density ratio sample period (see Figure 4.2). Ap data was obtained from Solar Geophysical Data over that same period plus the period back to January 1, 1979 (see Figure 4.2). In this test the Ap and PPE data used in correlation was available from 22.3 hours (15 sample periods) preceding day 79, which was the first day of the density ratio data.

Since the first test was to determine the amount of correlation between the two parameters and the density ratio, the data had to be linearly interpolated to the end time of the accelerometer sample period. In effect this put the two parameters on an equal time base to simplify the comparison. Furthermore, linear interpolation was applied because Ap is a linear representation of geomagnetic activity, and since the highly scattered PPE to Ap relationship is approximately linear (see section 4.1), we relate PPE linearly to geomagnetic activity.

Once the interpolation was complete the two parameters were correlated with the density ratio. As they stood, for the entire sample period (79/0233 UT - 100/2150 UT, 1979), the Ap and PPE gave linear-correlation coefficients of .47 and .42 respectively.

These somewhat low correlation coefficients were expected, since physically the upper atmosphere does not respond instantaneously to magnetospheric heat input (eg. Mayr and Volland, 1973) but acts as a slowly responding heat sink. Evidence has mounted over the years which demonstrates that a phase lag introduced to empirical models provides the best description of density changes as a result of varying geomagnetic conditions [eg. Marcos et al, 1977].

With this in mind, a program was run to correlate time-lagged parameters to the density ratio. The program was set up to step back or forward in time in order to determine the amount of time lag which would produce a maximum correlation coefficient. Due to the characteristic response time of the upper atmosphere to magnetospheric heat input, as described above, some sort of time lag to obtain a maximum correlation was expected.

The correlation plots of the first test are shown in Figures 4.5-4.8 and the results are summarized in Table 4.1. In each of the figures, the correlation coefficients are plotted as a function of sample period (approximately 1.5 hours). Also included are the first two standard deviations of the correlation coefficient (shaded region) which resulted from random numbers being linearly correlated with the same density ratio data within each sample period (this was done with the same correlation program, calling a random number generator for each sample). Also, to represent the uncertainties in the data, an error bar at maximum correlation shows two standard deviations of the linear-correlation coefficients where 50% gaussian random noise was introduced into the three data sets. The reason 50% was chosen was because it is difficult to define the uncertainty in the PPE and density ratio computations, and 50% was considered a reasonable estimate for this particular study (Marcos, Evans, private communication, 1988).

Table 4.1 provides the correlation coefficient (r) for both the Ap and PPE parameters at a lagged time to where the coefficient was a maximum. The "Lag" refers to the specific time which produced the maximum correlation coefficient (in all cases the maximum correlation occurred between the density ratio and a parameter value from a time preceding (lagging) the sampled data). Additionally, included in Table 4.1, is the probability "P" of obtaining such a coefficient from a completely uncorrelated population (for the FORTRAN program used see Bevington [1969]).

Figure 4.5 represents the entire sample period for test 1. The correlation coefficients for Ap remains somewhat larger than PPE

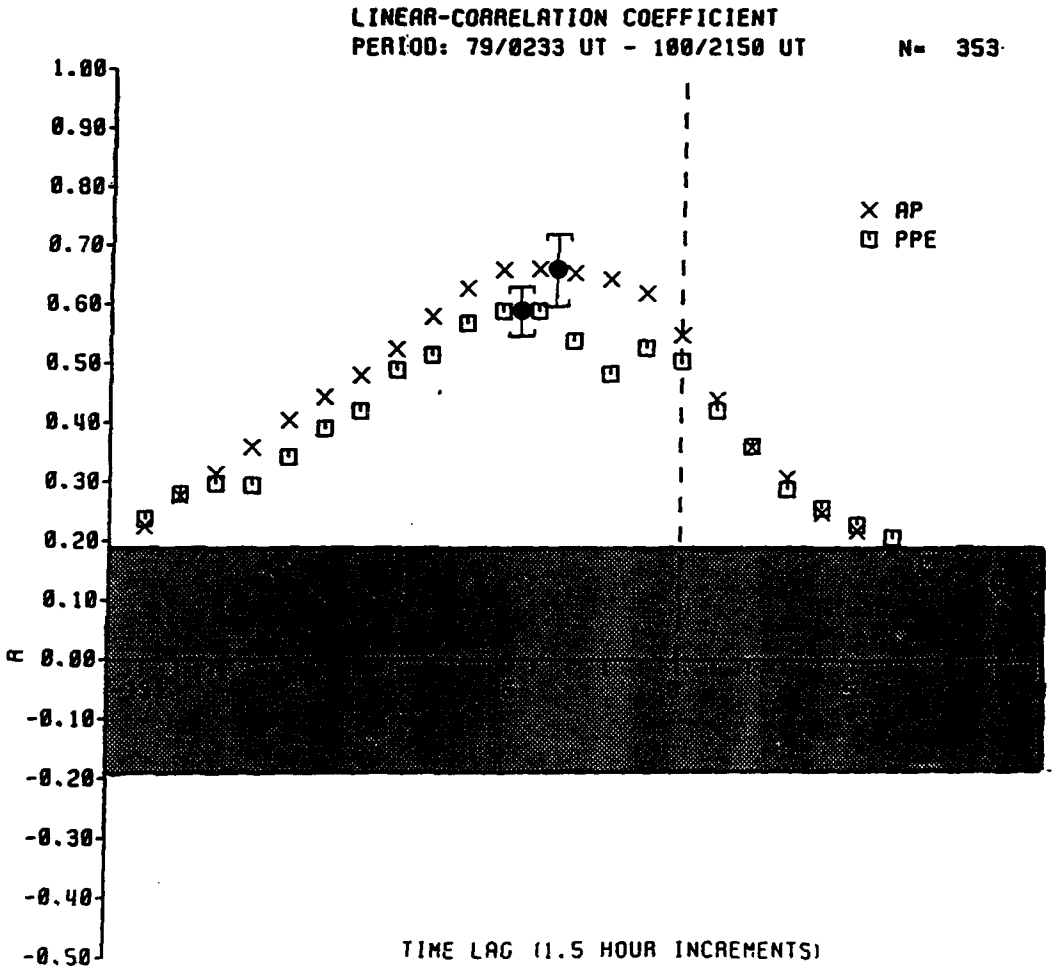

Fig. 4.5 Correlation coefficients for the entire sample period (1979 Julian days) between the density ratio, and both PPE and Ap, as a function of 1.5 hour increments.

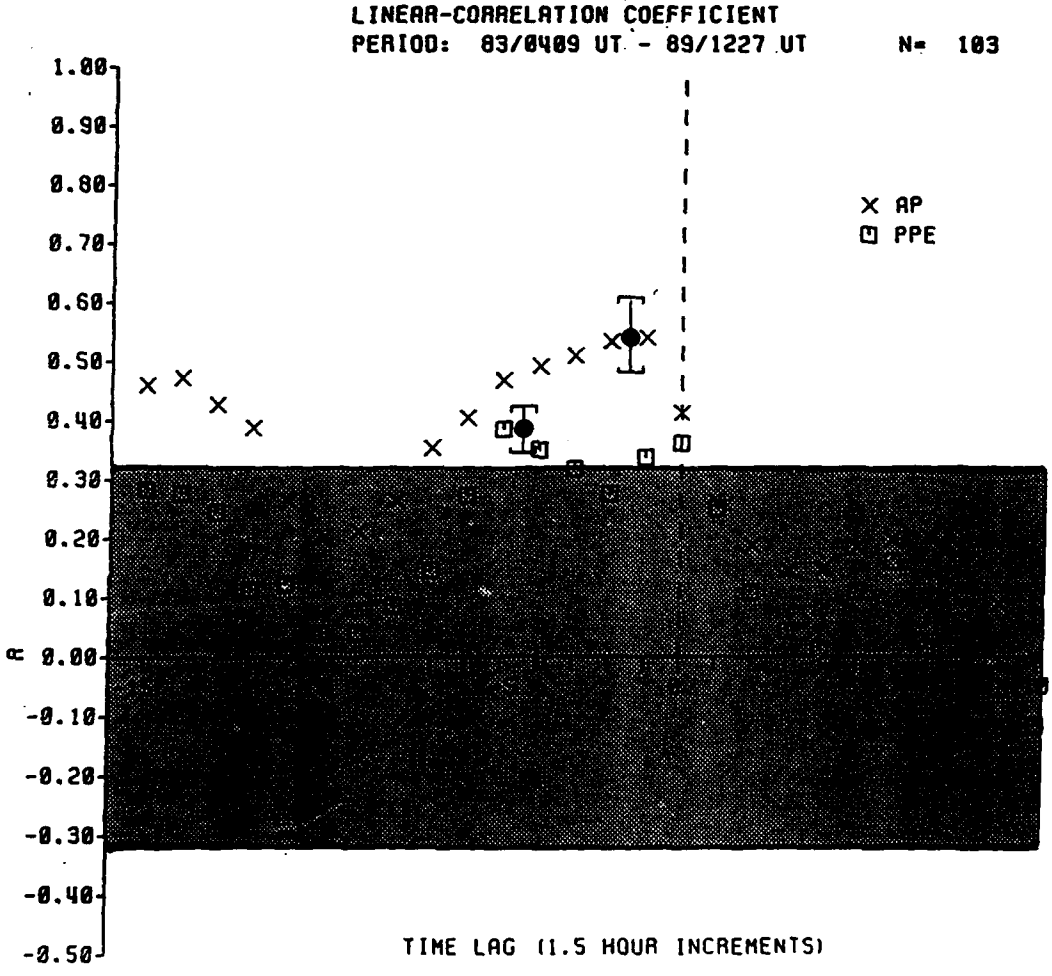

Fig. 4.6 Correlation coefficients for the first geomagnetically active period (1979 Julian days) between the density ratio, and both PPE and Ap, as a function of 1.5 hour increments.

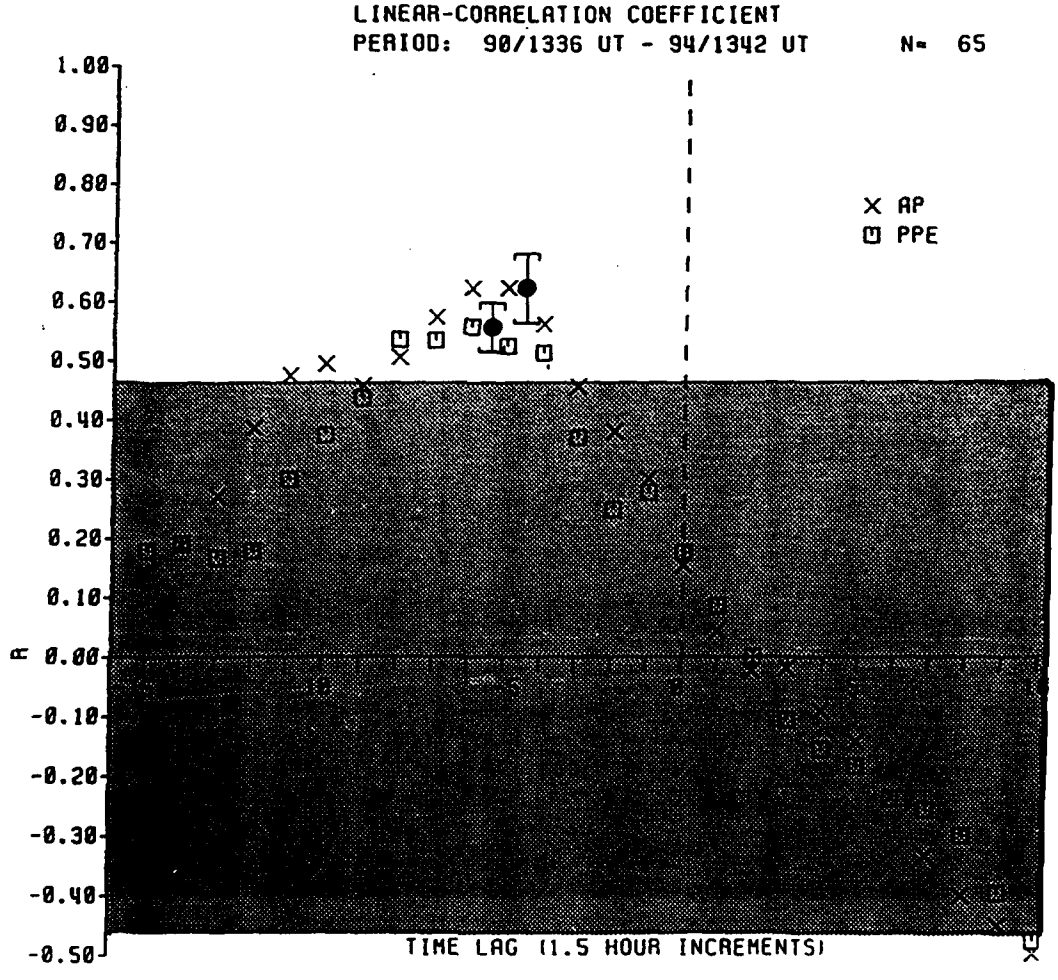

Fig. 4.7 Correlation coefficients for the second geomagnetically active period (1979 Julian days) between the density ratio, and both PPE and Ap, as a function of 1.5 hour increments.

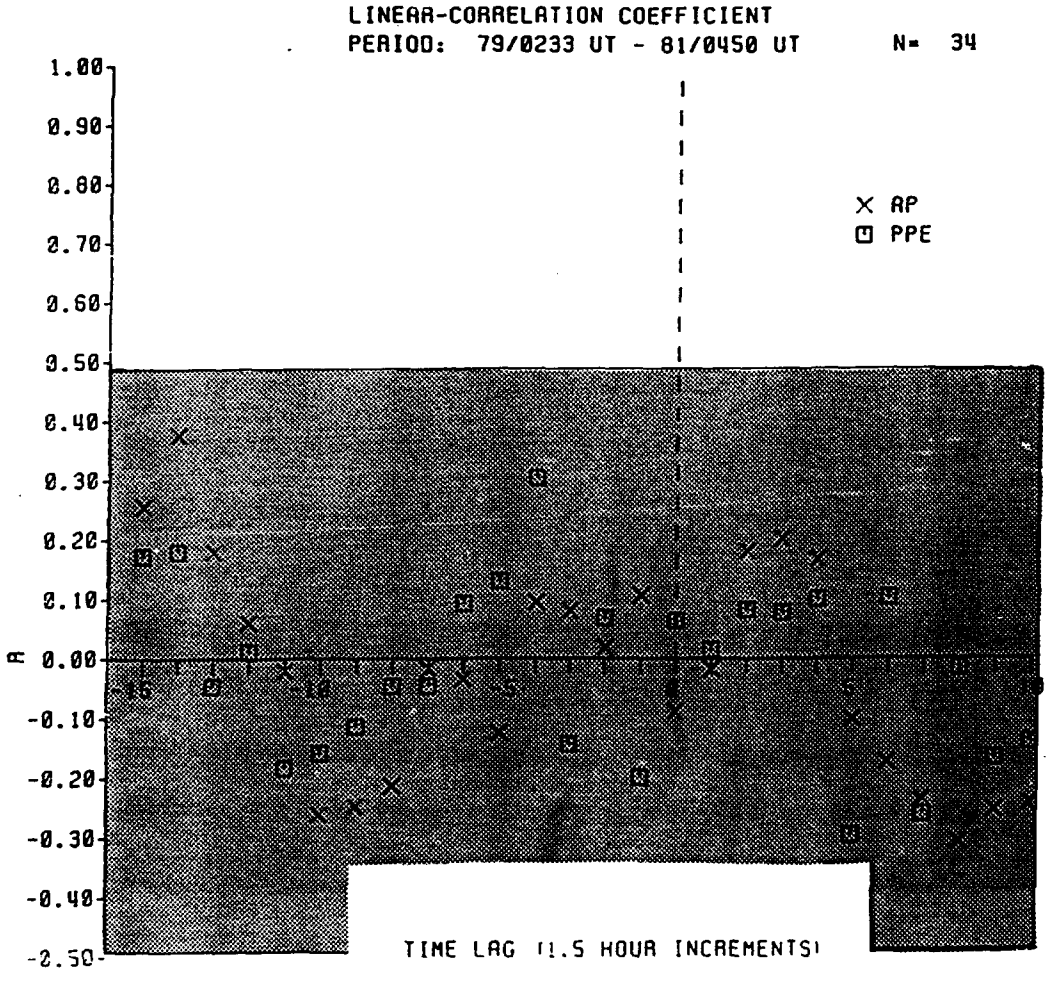

Fig. 4.8 Correlation coefficients for the geomagnetically quiet level period (1979 Julian days) between the density ratio, and both PPE and Ap, as a function of 1.5 hour increments.

throughout the period, but the sensitivity of the data at two standard deviations makes the two parameters indistinguishable in degree of correlation. Maximum peaks for Ap and PPE (.66 and .59 respectively) nearly correspond in time. An interesting feature of the PPE graph is the double peak. This behavior could be purely statistical or may be due to different characteristics which exist between geomagnetic storms. One further explanation may be the different response characteristics of direct heat input versus indirect ionization effects.

TABLE 4.1 Results of Density Ratio Correlations with Ap and PPE of the Periods Tested, Showing the Linear-Correlation Coefficients (r), Lag Time (Lag) of the Maximum Correlation, and the Probability (P) that r Could Come from a Completely Random Sample Population

Period	r_{Ap}	Lag (hours)	P	r_{PPE}	Lag (hours)	P
All	.66	6.0	7(-11)	.59	6.0	6(-11)
Active 1	.54	1.5	4(-9)	.38	7.5	7(-5)
Active 2	.62	7.5	4(-8)	.56	9.0	1(-6)

In conclusion, the correlation coefficients of PPE compared to Ap are statistically indistinguishable. Therefore, PPE is no better than Ap in describing the density fluctuations, at least in this particular period. However, the relative utility question is not yet answered by this result, when considering PPE is potentially available in real time [Evans, private communication, 1988], and this parameter has a definite disadvantage in spatial coverage when compared to the Göttingen Ap. These characteristics seem to indicate the potential of

this parameter, or an improved PPE parameter in surpassing the Ap as an index of magnetospheric activity. Furthermore, it was demonstrated that a time-delayed Ap or PPE provides a better parameter for describing the thermosphere's response to magnetospheric heat input, compared to the parameter without time delay. The time delay of the thermosphere's response is about 7.5 hours for this general period. However, the peak is very broad with a 4-hour spread, making this difficult to determine exactly.

Figure 4.6 represents the first isolated active period (Ap of 15 and above), from Day 83/0409 UT to Day 89/1227 UT. This first active period ranges from an Ap of 15 to a maximum Ap of 111, with PPE varying from 7 to 152 Gigawatts. In this period the relative comparison between the Ap and PPE correlation coefficients showed Ap to be the more highly correlated parameter ($r = .55$) than PPE ($r = .38$). Notice how much more complex and fluctuating the hemispheric power input throughout this active period is as compared to the Ap variability (see Figure 4.4).

Active Period 2 (Figure 4.7), which is from Day 90/1336 UT, to Day 94/1342 UT seems to behave more as expected, in contrast to the first active period. The range for the Ap index within this period is 15 to 207, with PPE ranging from about 8 to 160 Gigawatts. The lag times of maximum correlation of the two parameters virtually coincide, with maximum occurring at the 7 to 8 hours. The maximum correlation coefficient for Ap is .62, and PPE is .56. The difference in correlation coefficients is not as dramatic as in the previous case.

Figure 4.8 represents the only quiet ($Ap < 15$) period (79/0233 UT - 81/0450 UT) tested. The sample size of this period was only 34,

and, therefore, there is no meaningful correlation between the parameters and the density. Since this study has statistically insufficient data points for quiet-time periods, no attempt will be made to describe the relative utility of the two parameters during quiet periods. Table 4.1 summarizes the results of this first test.

Table 4.2 Time in Hours as a Function of Geometric Attenuation

T	Time (hours)
0.00	0.0
0.50	4.3
0.75	10.4
0.90	28.8

4.6.2 Correlations Using Time Weighted Ap

To provide a more physically meaningful representation of heat input into the thermosphere, it would be helpful to weight the parameters to make them more representative of how the atmosphere responds to heat input. As mentioned previously Marcos et al. [1977] have shown the 12-hour average of the Kp to be a better first-order approximation for this response characteristic than the nonaveraged value.

In this study further processing of Ap data was done, which Wrenn [1987] has shown to be helpful when describing ionospheric responses to changes in Ap. In his study, he presents a time-weighted Ap through the use of a three-hour attenuation multiplier T ($0 < T < 1$) applied

to a geometric progression. In producing such a geometric attenuation he introduces the factor (1-T) as a normalization factor since

$$Ap(T)=(1-T)[Ap + (T)Ap_{-1} + (T^2)Ap_{-2} + ...]$$

The application of T is equivalent to increasing the weight of the most recent index, while at the same time causing values to drop by a factor of 1/e in a time period which corresponds to the values listed in Table 4.1. For three-hour index values, Table 4.2 represents the time which corresponds to the attenuation factor T.

This attenuation was applied to the Ap data of 1979 by using the recurrence formula described by Wrenn [1987]. Figure 4.9 shows the effect that the weighting factor has on the Ap index throughout the 20-day test period, as well as days preceding and following this period. The first through the third panels represent the weighted Ap values which correspond to the 4.3, 10.4, and 28.8-hour attenuation listed in Table 4.2. This procedure filters the index to contribute a geometrically weighted effect into the future.

Figures 4.10 to 4.12 represent the time-weighted Ap correlation to the density ratio. On these graphs three weighted Ap indices are plotted, the unattenuated index, the Ap(T) with the T that produced the highest correlation, and an Ap(T) with T=.90 plotted on each graph to show the trend that the weighting introduces to the correlation.

From Figure 4.10 it appears that the introduction of a weighting function is advantageous. The improvement in the correlation over the entire period is about .08 (.74 verses .66) better than when using the unattenuated time-lagged value. This seems physically logical, since the upper atmosphere slowly responds to fluctuating magnetospheric heat input. Over the entire period, the optimum response time of the

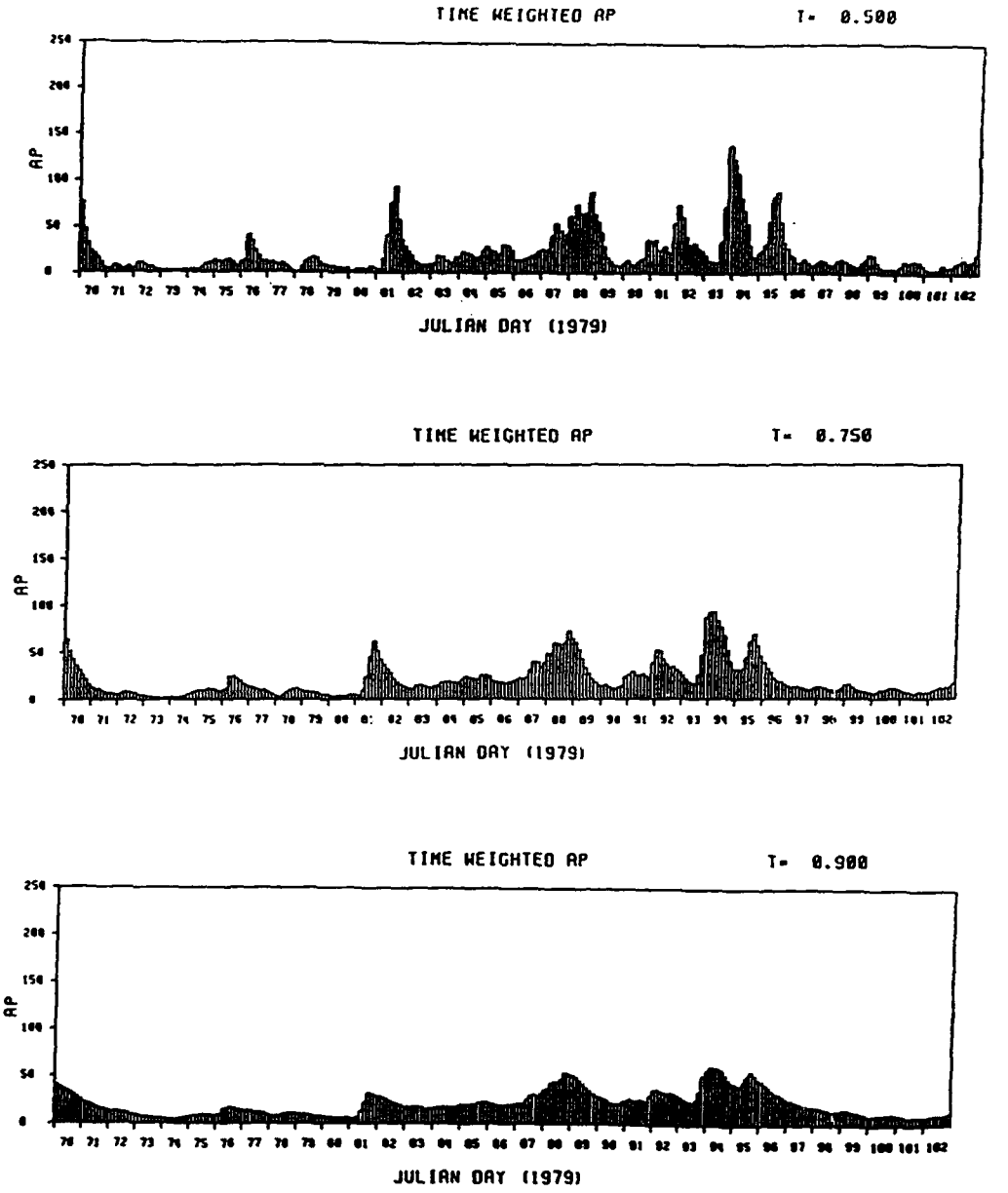

Fig. 4.9 The effect of geometric time weighting upon Ap. The first through third panels show attenuations of approximately 4.3 hours, 10.4 hours, and 1.2 days respectively.

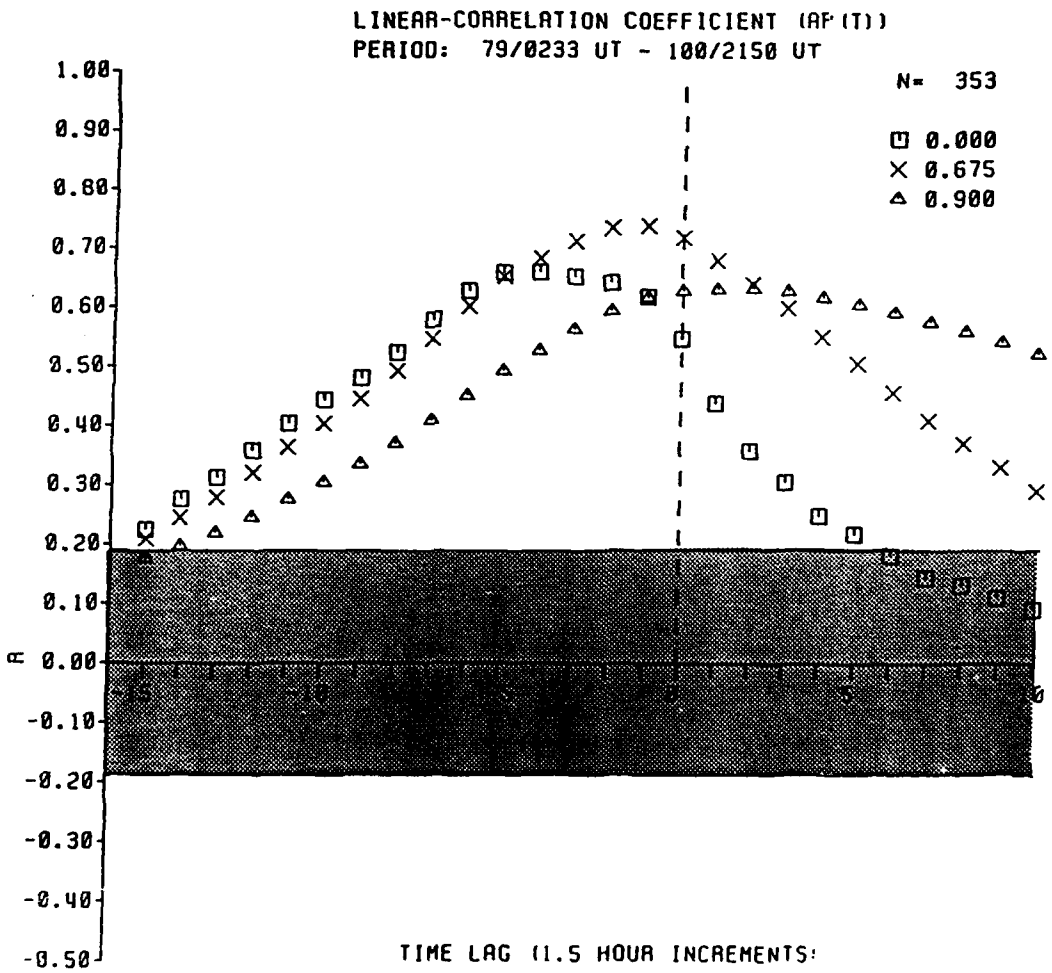

Fig. 4.10 Correlation coefficients for the entire sample period (1979 Julian days) between the density ratio, and the attenuated Ap at 0.0 hours, 1.2 days and where the attenuation produced the maximum correlation coefficient.

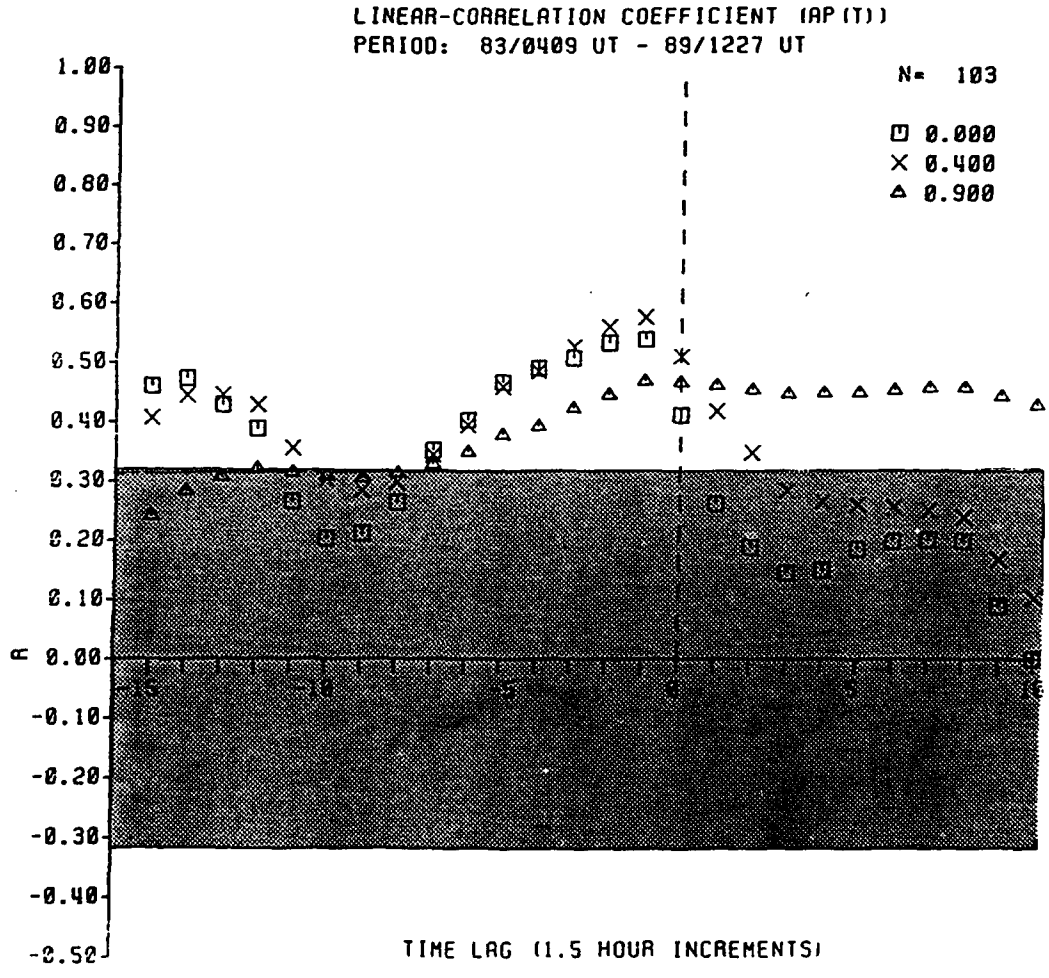

Fig. 4.11 Correlation coefficients for the first geomagnetically active period (1979 Julian days) between the density ratio, and the attenuated Ap at 0.0 hours, 1.2 days and where the attenuation produced the maximum correlation coefficient.

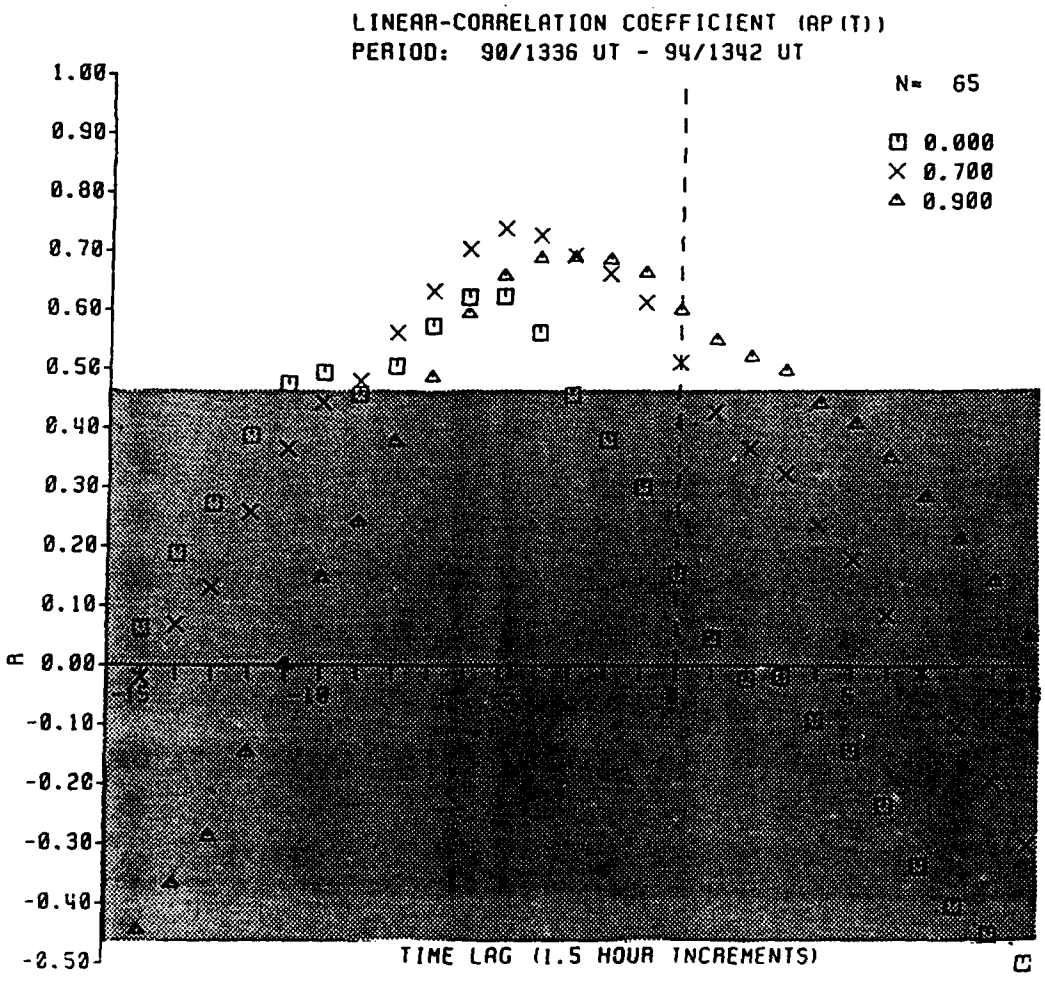

Fig. 4.12 Correlation coefficients for the second geomagnetically active period (1979 Julian days) between the density ratio, and the attenuated Ap at 0.0 hours, 1.2 days and where the attenuation produced the maximum correlation coefficient.

atmosphere uses a T of .675 or 7-9 hours. The improvement is significant.

Figure 4.11 confirms the complexity of the first active period. The improvement of the correlation is not as significant as for the overall period.

Figure 4.12 represents the second active period. The correlation is optimized with a T = .7 giving an r = .74. This shows a .14 improvement in the correlation coefficient over the maximum raw Ap coefficient. Table 4.3 summarizes the results of this second test.

TABLE 4.3 Results of Density Ratio Correlation with Ap(T), Showing the Attenuation Factor (T) Which Produced the Maximum Correlation (r) at the Lag Time (Lag) of the Maximum Correlation, and the Probability (P) that r Could Come from a Completely Random Sample Population

Period	T	r(T)	Lag (hours)	P
All	.675	.74	1.5	less than 10(-11)
Active 1	.400	.58	1.5	2(-10)
Active 2	.700	.74	7.5	less than 10(-11)

4.7 Conclusion

In conclusion, the first test shows that the current PPE has no better correlation to density ratio changes than the current Ap parameter (see Section 4.6.1 and Table 4.2). Over the entire period, and including the lagged values, the Ap index showed a slightly better correlation coefficient than did the PPE; however, sensitivity tests of the data showed there was no statistically significant difference. Upon breaking the data down into statistically significant active

periods, the Ap correlated slightly better than the PPE in the first active period, but in the second active period no statistically significant difference was found.

All of this information shows that, in its present form and during this sample period, the PPE index was not any more useful than the Ap index in describing upper-atmospheric density perturbations due to magnetospheric processes.

That is not to say that the PPE index does not have the potential to become a better index than Ap. On the contrary, this study indicates that this type of index has such potential. This is due to the very nature of the PPE data itself. As mentioned previously (see Section 3.3), the PPE data comes from a single-line integral of particle precipitation and an empirical determination of what is happening globally. This fact puts the data at a definite disadvantage when it comes to spatial coverage, as compared to the global coverage of the Ap index. Additionally, the Göttingen Ap is an after-the-fact (many days until all the data is collected) geomagnetic index, giving it further advantage over the "real time" PPE data. Finally, in spite of all of these disadvantages, the PPE still has a comparable correlation coefficient (only a .07 difference over the entire sample period) relative to the Ap.

A further optimization of the correlation was the subject of the second test. In order to test the response characteristics of the thermosphere to magnetospheric energy input, a more physically representative time weighted index was introduced (Ap(T)). This geometrically time-weighted parameter showed a consistent improvement in linear-correlation coefficients over all three samples (Table 4.3).

This test reaffirms the physical response characteristics of the thermosphere. This assertion is made not only because of the enhanced correlation coefficient, but also because "lag" time was dramatically decreased by maximizing the correlation coefficient. This means that the physics of the situation is better described with this type of time weighting than with the raw lagged parameter.

CHAPTER V

ORBITAL ANALYSIS STUDY

5.1 Introduction

This chapter is a presentation of a study carried out at Space Command in Colorado Springs, Colorado, in the fall of 1987. The study focused on the utility of hemispheric power input (PPE) as compared to the Air Force's Ap geomagnetic parameter for use in operational satellite orbital analysis.

The Air Force's Ap differs from the Göttingen Ap in that it utilizes only western hemisphere stations. It has an inherent statistical weighting factor to make it more representative of the Göttingen Ap and weights the data to emphasize high-latitude geomagnetic perturbations [Krause, personal communication, 1988]. The reason this Ap is used rather than the Göttingen Ap index is that it is available in "real time" and thus adds to the operational objective.

The test involves the use of a semianalytic orbital ephemeris generator [Liu, 1979] which uses an empirical upper-atmospheric density model in describing the state of atmospheric drag. This chapter begins with a description of the test conducted by the Space Command Astrodynamics group [Liu et al., 1982], which evaluated the operational utility of various empirical upper atmospheric density models as applied to the "real world" environment. The chapter concludes with a discussion of the same type of test applied to the two geophysical parameters, Ap and PPE.

5.2 Empirical Atmospheric Density Model Applications Study

To insure the accuracy of the state of the atmosphere at various altitudes, satellite orbital models utilize state-of-the-art empirical density models. In an operational evaluation of such density models Liu et al. [1982] conducted practical tests of various upper atmospheric density models through the use of orbital mechanics. More specifically, the orbital models used to test the upper atmospheric density models consisted of the semianalytic integration method [Liu, 1979] as well as special perturbation theory. It was pointed out that although the test was not intended for scientific purposes, the study did reveal the practical applicability of various density models in a U.S. Air Force Space Command environment. In other words, the test emphasized the practical usefulness of density models to provide the most effective and efficient means of providing upper-atmospheric density information to a numerical orbital generator.

In order to make objective comparisons of the operational applicabilities of the various density models, a standard testing procedure and criteria from which to base the evaluation was developed.

The data base used for the study consisted of a collection of radar observations of satellite range, range rate, azimuth and elevation measurements.

The orbital ephemeris generator determined to perform most efficiently and effectively was the semianalytic theory model. This model describes the atmospheric drag and the second through fourth

zonal harmonics of the Earth's gravitational potential. These two forces are combined into singly averaged equations of motion and subsequently numerically integrated to produce the required ephemeris.

The specific test cases chosen were satellites which had high density observational data bases. The orbits chosen were to be approximately twenty days prior to decay, which would provide samples with a maximum amount of atmospheric drag.

The test procedure applied to these cases was set up to emphasize how well the various density models performed in orbit determination, short-term prediction, and lifetime estimation when used by the ephemeris generator.

The test used six singly averaged initial orbital elements along with the appropriate ballistic coefficient and the classical least square differential correction technique [ADCOM, 1977] in order to fit the observational data (see Appendix for a general explanation of the differential correction method).

After orbit initialization, a short-term prediction was made using a given density model. The resulting prediction was then qualitatively evaluated in terms of the root mean square (RMS) of the position differences in km, and the difference at the end of the prediction span. The study concluded that Jachia 70 [1970] upper-atmospheric density model had the best overall performance.

5.3 Parameter Study

In this study, basically the same test was performed as was discussed in 5.2. The difference is that there was only one density model used, the Jachia 70 [1970], and the test was to determine

whether or not the introduction of the PPE index improves the RMS positional accuracy of the end time positional differences when compared to a run using the Air Force's Ap index. The hypothesis is that if this parameter were better in describing heat input to the thermosphere than the Ap index, the RMS of the positional difference would be lower for PPE than the Ap.

The particular test cases chosen for this study had high inclinations so as to emphasize auroral zone effects. They were also chosen because of their fairly low peregees, so as to maximize the drag effects.

Table 5.1 summarizes the initial condition ephemeris of the three test cases.

Table 5.1 Initial Ephemeris Conditions for Orbital Analysis Study

Sat No.	Apogee (km)	Perigee (km)	Inclination (deg)	Period (min)
11285	1010	509	74	100
11161	971	430	83	98
7337	1921	414	83	108

Table 5.2 is a summary of the RMS value to where the differential correction converged. This simply means that this was where the residual of the predicted position versus the observed position was found to be minimum. The smaller the RMS the more useful the density model is to the orbital model in making orbit determination.

As this table shows, of the satellites tested all three had their lowest RMS with Ap rather than PPE as the geomagnetic index. The consistent difference shows that the Ap may be the better parameter, and indicates that PPE in its present form is probably not as useful in orbital analysis as the Ap.

TABLE 5.2 Summary of RMS Residual from Orbital Analysis Study of the Operational Utility of Ap and PPE Magnetospheric Parameters

Satellite No.	PPE	Ap
11285	2.969	2.614
11161	5.973	5.215
7337	2.976	1.800

One must be very careful to qualify this statement, since what is being tested is a parameter (PPE) within an empirical model which has been built upon a different parameter (Ap). However, the test may be valid since the density model tries to track heat input through tracking an increase in the Ap index. If PPE is a valid physical parameter for the amount of heat input into the atmosphere, then it is possible that it could improve the model's performance as applied to orbital analysis, and it is in this context that the test was made.

Additionally, the RMS results are consistent with the accelerometer study conclusions, and may be further evidence that the PPE is no more useful in describing upper atmospheric density perturbations due to magnetospheric energy input than the currently used "Ap" index. However, the PPE results were favorable, and it may

be more fair to compare a PPE binned empirical model with other Ap binned models.

CHAPTER VI

CONCLUSIONS/RECOMMENDATIONS

The accelerometer study demonstrated the potential of global hemispheric power (PPE) as measured by the NOAA/TIROS satellite as a more useful parameter than Ap. This conclusion considers the potential operational availability of the PPE, as well as its disadvantage in spatial coverage (see Section 3.3), when compared to the Göttingen Ap. Even with the inherent difficulty in spatial coverage, the PPE and the Ap had statistically indistinguishable correlation coefficients when correlated with the accelerometer density data.

In view of this excellent performance it is suggested that an investigation of the operational implementation of this parameter be conducted. Furthermore, realizing the 10-year PPE data base which is available, it is advised that an empirical model be built using this rather than the Ap data base.

Additionaly, it is recommended that an improved PPE be developed by supplementing it with other auroral sampling satellite instruments such as DMSP or other new PPE-type satellite instruments. It is this author's hypothesis that an improved PPE would surpass the current Ap index in utility, as applied to modeling magnetospheric heat input to the thermosphere. This hypothesis could be tested through the same test employed in this study.

Additionally, since this study demonstrates the potential of a more physically representative magnetospheric parameter, it seems only logical to suggest the use of an auroral imager as an alternative to

the problem of having many satellites to provide adequate coverage of auroral processes.

This study also provided a look at a time-weighted Ap parameter, which improved not only the magnitude of the correlation coefficient but also significantly decreased the time lag to the maximum correlation coefficient. This supports the theory that the thermosphere responds in an integrated, rather than instantaneous, fashion to magnetospheric heat input. This observation could motivate a further investigation of this type of weighting to current geomagnetic indices or possibly the development of a new PPE type index, as they both apply to neutral upper atmospheric density modeling.

Finally, this study showed that there may be an upper limit to the capability of a magnetospheric parameter to model perturbations in satellite drag, because current models do not contain wind and chemistry-induced affects. Additionally, due to the complicated magnetospheric system, a single magnetospheric parameter probably is incapable of precisely modeling Joule dissipation.

The second study demonstrated that, in the cases tested, the operational applicability of the PPE index in its present form is no better than the Air Forces real time Ap index. However, caution must be applied to this conclusion since the empirical model to which the PPE was entered and which was used by the orbital model was binned using the Ap index. Even with this disadvantage PPE still obtained favorable results. Additionally, to make the test more fair, it is recommended that an empirical model based upon PPE be tested in the same manner.

The following is a summary of the recommendations of this research:

1. Investigate the implementation of the PPE parameter for operational use.

2. Build new empirical upper atmospheric density models based upon the existing 10-year PPE data base.

3. Develop an improved PPE parameter by supplementing NOAA/TIROS data with other auroral particle instruments (e.g., DMSP).

4. Test this new model against Ap-binned models in other orbital model studies.

5. Investigate thermospheric density modeling using improved existing parameters (e.g., time-weighted Ap).

6. Use imaging satellites to improve spatial coverage of magnetospheric energy input, and develop models based on this new data base.

7. Further investigate the limit of the optimization of magnetospheric parameters associated with the affects of winds, chemistry, and Joule heating as these phenomena relate to satellite drag modeling.

REFERENCES

ADCOM, Mathematical Foundation for SCC Astrodynamic Theory, Space Computational Center Program Documentation, ADCOM DCD8, Peterson AFB CO, 5-1, September, 1977.

Bahnsen, A., Recent techniques of observations and results from the magnetopause regions, J. Atmos. Terr. Phys., 40, 235-256, 1978.

Banks, P. M., Energy sources of the high latitude upper atmosphere, in Exploration of the Upper Atmosphere, edited by C. S. Deehr, J. Hollet, and D. Reidel, Hingham, Mass., 1980.

Bate, R. R., et al., Fundamentals of Astrodynamics, Dover Publications Inc., New York, 1971.

Baumjohann, Merits and limitations of the use of geomagnetic indices in solar wind-magnetospheric coupling studies, in Solar Wind-magnetosphere Coupling, edited by Y. Kamide and J. A. Slavin, TERRAPUB, Tokyo, 3-15, 1986.,

Bevington, P. R., Data Reduction and Error Analysis for the Physical Sciences, McGraw-Hill, New York, 1969.

Cosmical Geophysics, edited by A. Egeland, O. Holter, and A. Omholt, Universitetsfolaget, Oslo, Norway, 1973.

Coster, A. J., and E. M. Gaposchkin, Evaluation of new parameters for use in atmospheric models, AAS Paper, 87-555, 1987.

Frank, L. A., et al., Global auroral imaging instrumentation for the Dynamics Explorer mission, in Dynamics Explorer, edited by R. A. Hoffman and D. Reidel, Dordrecht, Holland, 1981.

Hedin, A. E., MSIS-86 thermospheric model, J. Geophys. Res., 92, 4649-4662, 1987.

Jacchia, L. G., Corpuscular radiation and the acceleration of artificial satellites, Nature, 183, 1662, 1959.

Jacchia, L. G., Satellite drag during the events of November 1960, Space Research II, North-Holland Publ. Co., Amsterdam Holland, 747-750, 1961.

Jacchia, L. G., New satellite models of the thermosphere and exosphere with empirical temperature profiles, SAO SP-313, May 6, 1970.

Jacchia, L. G., Thermospheric temperature density and composition: new models, SAO SP-375, March 1977.

Jacchia, L. G., et al., Geomagnetic perturbations and upper atmospheric heating, J. Geophys. Res., 72, 1423-1434, 1967.

Lange, W. L., Development, Test, and Calibration of a Three-Axis Accelerometer Stystem, AFGL-TR-78-0003, Air Force Geophysics Laboratory, Hanscom AFB, Mass., December, 1977.

Liu, J. J. F., Semianalytic theory for a close-earth artificial satellite, J. Guidance and Control, 3, 304-311, 1979.

Liu, J. J. F., et al., An analysis of the use of empirical atmospheric density models in orbital mechanics, in Proceedings of a Workshop on Satellite Drag, NOAA, March 18-19, 1982.

Maeda, S., T. J. Fuller-Rowell, D. S. Evans, and J. C. Foster, Numerical simulations of thermospheric disturbances excited by magnetospheric energy input, 1984.

Marcos, et al., Density variations in the lower thermosphere from analysis of the AE-C accelerometer measurements, Planet. Space Sci., 25, 499-507, 1977.

Marcos, F. A., Application of satellite accelerometer data to improve density models, 1984.

Mayr, H. G., and H. Volland, Magnetic storm characteristics of the thermosphere, J. Geophys. Res., 78, 2251-2264, 1973.

NASA, Solar Terrestrial Physics: Present and Future, Edited by D. M. Butler and K. Papadopoulos, NASA Reference Publication 1120, University of Maryland, College Park Maryland, 1984.

Rees, M. H., et al., Neutral and ion gas heating by auroral electron precipitation, J. Geophys Res., 88, 6289-6300, 1983.

Richmond, A. D., Thermospheric dynamics and electrodynamics, in Solar Terrestrial Physics, edited by R. L. Carovillano and J. M. Forbes, 523-607, 1982.

Romick, G. J., The detection and study of the visible spectrum of the aurora and airglow, SPIE, 91, 63, 1976.

Seale, R. A., and R. H. Bushnell, The TIROS-N/NOAA A-J Space Environment Monitor Subsystem, NOAA Technical Memorandum ERL SEL-75, April 1987.

Wrenn, G. L., Time-weighted Accumulations ap(t) and Kp(t), J. Geophys. Res., 92, 10,125-10,129, 1987.

APPENDIX

Appendix: General Summary of the
Differential Correction Method

The following summary is taken out of Fundamentals of Astrodynamics by Bate et al. [1971], and is intended to give the reader a general outline of the differential correction method and the concept of residuals.

Differential correction utilizes the concept of residuals. A residual is defined as the difference between an actual observation and what that observation would have been if the satellite traveled along a theoretically nominal orbit. Due to the fact that satellite sensors have inherent errors in tracking, or because of uncertainty in the original observing station's geographic location, the station downrange may pick up different data than what was predicted.

Suppose one breaks a satellite's initial position r_i and velocity v_i into its resulting three dimensional components, and these six components describe the preliminary orbital elements of this satellite this epoch time t_i. Now assuming that a theoretical prediction is made as to the future position of this satellite at six different times, say t_1, t_2, t_3, t_4, t_5, and t_6. This prediction assumes that the initial observations were correct.

Furthermore, suppose that a downrange station makes observations of range rate at these same six prediction times and computes the residuals in the six age rates as

$$\Delta\dot{\rho}_1,\ \Delta\dot{\rho}_2,\ \Delta\dot{\rho}_3,\ \Delta\dot{\rho}_4,\ \Delta\dot{\rho}_5,\ \text{and}\ \Delta\dot{\rho}_6.$$

Assuming the residuals are small the following six first order equations may be written:

$$\dot{\Delta\rho}_1 = \frac{\partial \dot{\rho}_1}{\partial r_I} \Delta r_I + \frac{\partial \dot{\rho}_1}{\partial r_J} \Delta r_J + \frac{\partial \dot{\rho}_1}{\partial r_K} \Delta r_K + \frac{\partial \dot{\rho}_1}{\partial r_I} \Delta r_I + \frac{\partial \dot{\rho}_1}{\partial r_J} \Delta r_J + \frac{\partial \dot{\rho}_1}{\partial r_K} \Delta r_K$$

$$\vdots \qquad \vdots \qquad \vdots \qquad \vdots \qquad \vdots \qquad \vdots \qquad \vdots$$

$$\dot{\Delta\rho}_6 = \frac{\partial \dot{\rho}_6}{\partial} \Delta r_I + \frac{\partial \dot{\rho}_6}{\partial r_J} \Delta r_J + \frac{\partial \dot{\rho}_6}{\partial r_K} \Delta r_K + \frac{\partial \dot{\rho}_6}{\partial r_I} \Delta r_I + \frac{\partial \dot{\rho}_6}{\partial r_J} \Delta r_J + \frac{\partial \dot{\rho}_6}{\partial r_K} \Delta r_K$$

Where I, J, K represent orthoganal coordinates.

Assuming that the partial derivatives in this equation may be evaluated, this equation may be represented by a set of six simultaneous linear equations in six unknowns, Δr_I, Δr_J, Δr_K, Δv_I, Δv_J, Δv_K. Using matrix methods this equation can be solved for correction terms which are then added to the initial prediction terms to produce an "improved" set of orbital elements

$$[r_I + \Delta r_I,\ r_J + \Delta r_J, \ldots\ldots, v_K + \Delta v_K].$$

These corrected values are then used to produce a new "updated" prediction of six new range rates. The resulting residuals from this new prediction are the used in the same process until convergence to a smallest value residual is obtained. This then is basically an six dimensional iterative technique where trial and error is used to determine the orbital elements which would reduce the residual to zero. For further information on the general differential correction technique see Bate et al [1971]. For information concerning the specific technique used by Space Command Astrodynamics see ADCOM DCD8, [1977].

VITA

Kelly Jon Hand

Candidate for Degree of

Master of Science

Thesis: Determination of the Utility of Hemispheric Power Input as a Parameter of Upper Atmospheric Density Modeling as Applied to Satellite Orbital Analysis

Major Field: Soil Science and Biometeorology

Biographical Information:

PII Redacted

Personal Data: [redacted], son of August and Leanne Hand; married Cindy Ann McDonald, August 13, 1977; three children--Joshua, Lindsay, and Hillary.

Education: Graduated from Fairmont High School in 1975; obtained a Bachelor of Science Degree from Mankato State University in 1980; in December of 1981, graduated with a Basic Meteorology Degree under Air Force Institute of Technology sponsorship at Texas A and M University.

Professional Experience: Space Environment Analyst at the North American Aerospace Defense Command (NORAD), Cheyenne Mountain Complex, Weather and Solar Support Unit, Fourth Weather Wing in Colorado Springs Colorado; Technique Development Officer at Operating Location B, Air Force Global Weather Central, Space Environment Services Center, Space Environment Laboratory in Boulder Colorado.